Electronic Supplementary Information

Dynamic Dimer-Monomer Equilibrium in a Cycloruthenated Complex of $[Re(\eta^6\text{-}C_6H_6)_2]^+$

Daniel Hernández-Valdés, Lionel Wettstein, Ricardo Fernández-Terán, Benjamin Probst, Thomas Fox, Bernhard Spingler, Qaisar Nadeem and Roger Alberto*

Department of Chemistry, University of Zurich, Winterthurerstr. 190, CH-8057 Zürich, Switzerland.
*E-mail: ariel@chem.uzh.ch. Phone: 0041 44 635 46 31

Table of Content

1. General Information

a. Materials

All reactions were carried out under nitrogen atmosphere on a standard nitrogen/vacuum line. The glassware was dried by the use of a heat gun or in an oven at 130 °C. Commercially available reagents were purchased reagent-grade and used without further purification. All chemicals were purchased from Sigma Aldrich (Switzerland). The chemicals were used without further purification. Deuterated NMR solvents were obtained from Armar Chemicals (Switzerland).

b. Characterization

FT-IR spectra were acquired on a Perkin Elmer Spectrum Two spectrophotometer equipped with a Specac Golden Gate single reflection diamond accessory. FT-IR spectra in solution were recorded in CD_3CN using

a Bruker Vertex 80v spectrometer purged with dry nitrogen during measurements, in a home-built flow cell with two 2 mm CaF_2 windows and a 100 µm Teflon spacer, with the pure solvent as background.

^{1}H NMR, $^{13}C\{^{1}H\}$-NMR and DEPT-NMR spectra were recorded on Bruker DRX 400 MHz or 500 MHz spectrometers. ^{1}H and ^{13}C chemical shifts were referenced to the residual solvent resonances, relative to TMS.

Preparative HPLC was performed on a Varian ProStar 320 system, using a Dr. Maisch Reprosil C18 100-7 (40 x 250 mm) column. The solvents (HPLC grade) were 0.1% trifluoroacetic acid (solvent A) and acetonitrile (solvent B). Analytical HPLC was performed on a VWR HITACHI Chromaster system, using a Macherey-Nagel Nucleosil C18 100-5 column. HPLC solvents were 0.1 % trifluoroacetic acid or 0.1 % formic acid (solvent A) and acetonitrile (solvent B).

Electrospray-ionisation mass spectrometry (ESI-MS) was performed on a Bruker esquireTM/LC spectrometer or a Bruker esquireTM/HCTTM spectrometer. High-resolution mass spectrometry (HR-ESI-MS) was performed on a Bruker maXis QTof high-resolution mass spectrometer (Bruker GmbH, Bremen, Germany).

UPLC-ESI-MS was performed on a Waters Acquity UPLC system coupled to a Bruker HCTTM, using an Acquity UPLC BEH C18 1.7 µm (2.1 x 50 mm) column. UPLC solvents were formic acid (0.1% in millipore water) (solvent A) and acetonitrile HPLC grade (solvent B). Applied UPLC gradient: 0-0.5 minutes: 95% A, 5% B; 0.51-4.0 minutes: linear gradient from 95% A (5% B) to 0% A (100% B); 4-5 minutes: 100% B. The flow rate was 0.6 ml/min. Detection was performed between 250 nm and 480 nm (DAD).

X-ray Crystallographic data were collected at 183(2) K with Mo Kα radiation (λ = 0.7107 Å). Compounds were measured on a Rigaku-Oxford Diffraction, dual source, XtaLAB Synergy system with a Dectris Pilatus3 R 200K detector. Suitable crystals were covered with oil (Infineum V8512, formerly known as Paratone N), placed on a nylon loop that is mounted in a CrystalCap Magnetic™ (Hampton Research) and immediately transferred to the diffractometer. Data were corrected for Lorentz and polarization effects as well as for absorption (numerical). The program suite $CrysAlis^{Pro}$ was used for data collection, multi-scan absorption correction and data reduction.[1] Structures were solved with direct methods using ShelxT[2] and were refined by full-matrix least-squares methods on F^2 with SHELXL-2014.[3] The structures were checked for higher symmetry with the help of the program Platon.[4] CCDC 2007155-2007157 contain the supplementary crystallographic data for this paper. These data are provided free of charge by The Cambridge Crystallographic Data Centre *via* www.ccdc.cam.ac.uk/structures.

2. Synthetic procedures and analytical data

[Re(η⁶-C₆H₅C(CH₃)(OH)(C₅H₄N))(η⁶-C₆H₆)](PF₆) ([2](PF₆))

[Re(η⁶-C₆H₅C(CH₃)(OH)(C₅H₄N))₂](PF₆) ([3](PF₆))

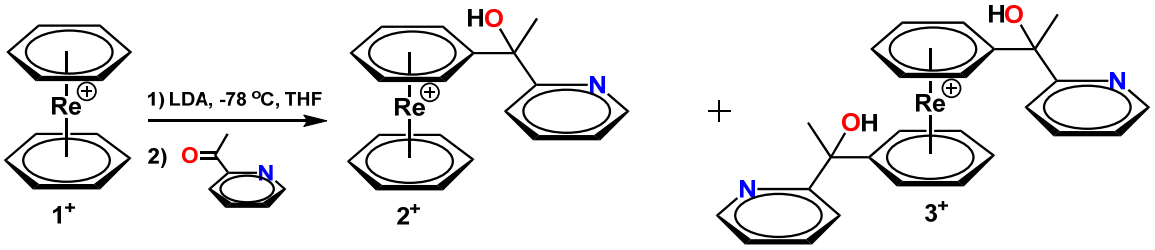

Synthesis: 125 mg (0.254 mmol, 1 eq.) **[1]**OTf was dissolved in 15 mL dry THF and cooled to -78 °C. Afterward, 0.8 mL (0.8 mmol, 3.2 eq.) of a 1 M LDA (THF/hexane) was slowly added to the yellow suspension, changing the color to dark orange. The reaction mixture was stirred for 75 min at -78 °C. Upon the addition of 385 µL (3.43 mmol, 13.4 eq.) of 2-acetylpyridine, the reaction mixture turned light orange. After stirring at -78 °C for 3 h, the reaction was quenched by the addition of 0.1 % aq. HTFA (2 mL) and the crude product was dried under N_2-stream. The solid residue was washed with Et_2O (4 × 5 mL) and then dissolved in ACN (2 mL) and H_2O (2 mL). Purification was done by prep-HPLC (Reprosil 100 C18, 250 mm × 40 mm, 0.1 % formic acid/ACN, gradient: 5 % ACN for 20 min, 5-50 % ACN in 45 min, 50-100 % ACN in 5 min). Yield: 58.2 mg (0.096 mmol, 38 %) for [Re(η⁶-C₆H₅C(CH₃)(OH)(C₅H₄N))(η⁶-C₆H₆)](PF₆), 64.2 mg (0.088 mmol, 35%) for [Re(η⁶-C₆H₅C(CH₃)(OH)(C₅H₄N))₂](PF₆). Complex **2**⁺ was obtained as a racemic mixture and **3**⁺ as a mixture of three stereoisomers (*SS*, *RR* and the meso). The three stereoisomers were partially separated in the prep-HPLC. The analysis was done with a pure sample containing only one of the isomer, but it was not possible to determine which one.

Analysis:

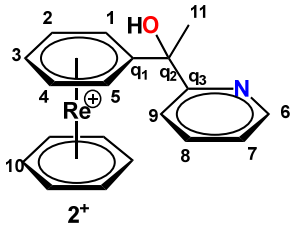

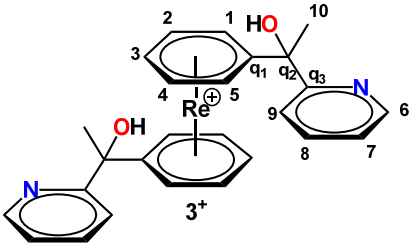

[Re(η⁶-C₆H₅C(CH₃)(OH)(C₅H₄N))(η⁶-C₆H₆)](PF₆) (**[2]**(PF₆)): ^{1}H NMR (500 MHz, CD_3CN) δ [ppm]: 8.57 (d, 1H, H_6), 7.85 (td, 1H, H_8), 7.64 (dt, 1H, H_9), 7.34 (ddd, 1H, H_7), 6.45 (d, 1H, H_1), 6.05 (d, 1H, H_5), 5.95 (t, 1H, H_2), 5.86 (t, 1H, H_3), 5.83 (s + t, 7H, $H_{10,}$ H_4), 1.80 (s, H_{11}); ^{13}C NMR (125 MHz, CD_3CN) δ [ppm]: 163.08 (C_{q3}), 148.88 (C_6), 138.65 (C_8), 124.21 (C_7), 121.02 (C_9), 106.73 (C_{q1}), 78.06 (C_{10}), 76.84 (C_1), 76.52 (C_3), 76.44 (C_4),

76.32 (C_2), 76.12 (C_5), 75.27 (C_{q2}), 29.85 (C_{11}). IR ν: 3093 (w), 1592 (w), 1571 (w), 1467 (m), 1399 (w), 1299 (w), 1198 (w), 1130 (w), 1066 (w), 1042 (w), 997 (w), 925 (w), 821 (s), 785 (m), 684 (w), 640 (w), 620 (w) cm^{-1}; HR-ESI-MS $C_{19}H_{19}ONRe$ $[M]^+$: calculated, 462.09907; found, 462.09948.

$[Re(\eta^6\text{-}C_6H_5C(CH_3)(OH)(C_5H_4N))_2](PF_6)$ (**[3]**(PF_6)): ^1H NMR (500 MHz, CD_3CN) δ [ppm]: 8.57 (d, 2H, H_6), 7.86 (td, 2H, H_8), 7.64 (d, 2H, H_9), 7.35 (m, 2H, H_7), 6.30 (d, 2H, H_1), 6.06 (d, 2H, H_5), 5.87 (t, 2H, H_2), 5.78 (t, 2H, H_3), 5.63 (t, 2H, H_4), 1.78 (s, 6H, H_{10}); ^{13}C NMR (125 MHz, CD_3CN) δ [ppm]: 163.06 (C_{q3}), 148.88 (C_6), 138.72 (C_8), 124.22 (C_7), 121.00 (C_9), 106.78 (C_{q1}), 77.21 (C_1), 77.14 (C_3), 77.08 (C_4), 76.98 (C_2), 76.92 (C_5), 75.42 (C_{q2}), 30.01 (C_{10}). IR ν: 3089 (w), 2984 (w), 2928 (w), 1592 (w), 1571 (w), 1471 (w), 1435 (w), 1399 (w), 1371 (w), 1299 (w), 1194 (w), 1154 (w), 1134 (w), 1070 (w), 1046 (w), 993 (w), 834 (s), 785 (m), 753 (m), 684 (w), 644 (w), 620 (w) cm^{-1}; HR-ESI-MS $C_{26}H_{26}O_2N_2Re$ $[M]^+$: calculated. 583.15185; found, 583.15222.

$[Ru(CO)_2Cl_2]_n$

Synthesized according to literature.[5]

$[Re(\eta^6\text{-}C_6H_6)(\eta^6\text{-}o\text{-}C_6H_4C(CH_3)(OH)(C_5H_4N)Ru(CO)_2(HTFA))](TFA)$ ([4a](TFA) and [4b](TFA))

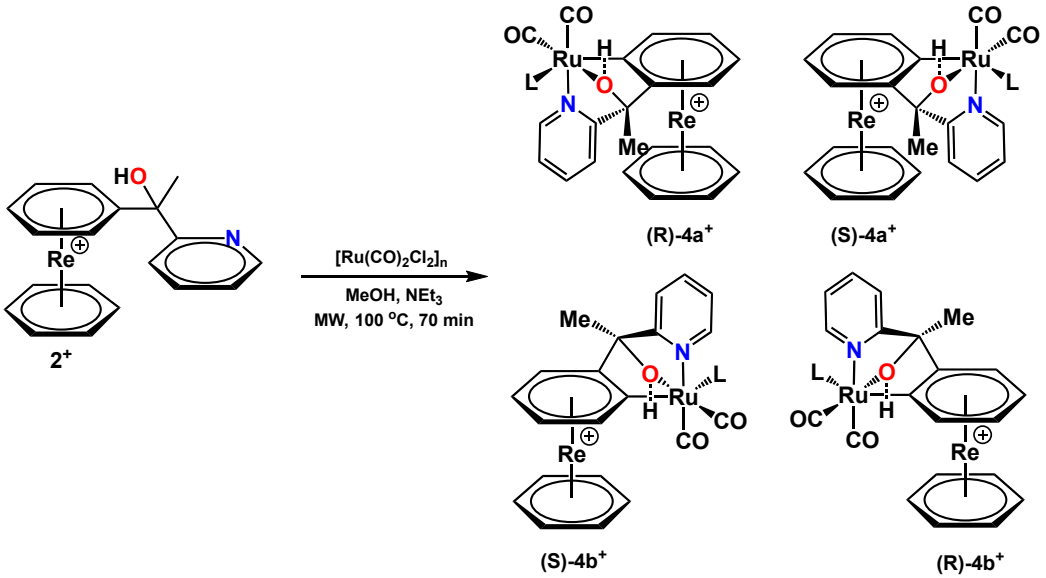

Synthesis: $[Ru(CO)_2Cl_2]$ (75 mg, 0.329 mmol, 3.43 eq.) was dissolved in NEt_3 (4 mL) and MeOH (4 mL) in a microwave vial. **[2]**TFA (58.6 mg, 0.096 mmol, 1 eq.) was added. The reaction mixture was kept at 100 °C for 70 min in the microwave. The solvent was removed under N_2-stream and the product was purified by prep. HPLC (Reprosil 100 C18, 250 mm × 40 mm, 0.1% HTFA/ACN, gradient: 10-40% ACN in 45 min, 40-

100% in 15 min, 100% ACN for 15 min). Isolated yield: 7.4 mg (0.0096 mmol, 10 %) for **[4a]**TFA and 18.5 mg (0.024 mmol, 25 %) for **[4b]**TFA.

Analysis: [Re(η^6-C_6H_6)(η^6-*o*-$C_6H_4C(CH_3)(OH)(C_5H_4N)Ru(CO)_2$(HTFA))](TFA) **[4a]**(TFA): ^{1}H NMR (CD_3CN, 500 MHz): 8.87 (d, 1H, C*H*$_{pyridine}$), 8.25 (t, 1H, C*H*$_{pyridine}$), 7.72 (d, 1H, C*H*$_{pyridine}$), 7.60 (t, 1H, C*H*$_{pyridine}$), 6.36 (d, 1H, C*H*$_{arene}$), 6.24 (d, 1H, C*H*$_{arene}$), 5.86 (t, 1H, C*H*$_{arene}$), 5.66 (t, 1H, C*H*$_{arene}$), 5.10 (s, 6H, C*H*$_{pyridine}$)(small singlet at 5.07 corresponding to 6H$_{arene}$ from partial dimerization), 2.18 (s, 3H, C*H*$_3$). The singlet at 1.96 could be assigned to non-deuterated acetonitrile coordinated to Ru; ^{13}C NMR (CD_3CN, 125 MHz): 196.36 (*C*O), 195.55 (*C*O), 165.22 (*C*$_{pyridine}$), 153.41 (*C*H$_{pyridine}$), 142.33 (*C*H$_{pyridine}$), 126.22 (*C*H$_{pyridine}$), 122.31 (*C*H$_{pyridine}$), 115.39 (*C*$_{arene}$), 110.02 (*C*$_{arene}$), 88.21 (*C*), 85.32 (*C*H$_{arene}$), 76.52 (*C*H$_{arene}$), 76.47 (*C*H$_{arene}$), 76.03 (*C*H$_{arene}$), 75.75 (*C*H$_{arene}$), 74.76 (*C*H$_{arene}$), 21.56 (*C*H$_3$). IR (solid sample): 3201 (w), 3093 (w), 2995 (w), 2058 (m, C≡O), 1989 (m, C≡O), 1675 (s, C=O, TFA), 1435 (m), 1190 (s), 1131 (s), 836 (m), 797 (m), 724 (m). IR (solution): 2070 (symmetric $\nu_{C\equiv O}$), 2001 (antisymmetric $\nu_{C\equiv O}$). HR-ESI-MS (MeCN): $C_{21}H_{17}O_3NReRu$; $[M]^+$; calculated, 619.97930; found, 619.98050.

[Re(η^6-C_6H_6)(η^6-*o*-$C_6H_4C(CH_3)(OH)(C_5H_4N)Ru(CO)_2$(HTFA))](TFA) **[4b]**(TFA): ^{1}H NMR (CD_3CN, 500 MHz): 8.73 (d, 1H, C*H*$_{pyridine}$), 8.09 (td, 1H, C*H*$_{pyridine}$), 7.78 (d, 1H, C*H*$_{pyridine}$), 7.48 (ddd, 1H, C*H*$_{pyridine}$), 6.25 (d, 1H, C*H*$_{arene}$), 6.11 (d, 1H, C*H*$_{arene}$), 5.93 (s, 6H, C*H*$_{arene}$), 5.73 (t, 1H, C*H*$_{arene}$), 5.67 (t, 1H, C*H*$_{pyridine}$), 2.05 (s, 3H, C*H*$_3$). The singlet at 1.96 could be assigned to non-deuterated acetonitrile coordinated to Ru; ^{13}C NMR (CD_3CN, 125 MHz): 196.75 (*C*O), 196.43 (*C*O), 161.63 (*C*$_{pyridine}$), 153.86 (*C*H$_{pyridine}$), 142.09 (*C*H$_{pyridine}$), 125.99 (*C*H$_{pyridine}$), 121.95 (*C*H$_{pyridine}$), 116.81 (*C*$_{arene}$), 108.01 (*C*$_{arene}$), 87.63 (*C*), 86.82 (*C*H$_{arene}$), 77.24 (*C*H$_{arene}$), 76.22 (*C*H$_{arene}$), 75.51 (*C*H$_{arene}$), 74.01 (*C*H$_{arene}$), 20.32 (*C*H$_3$). IR (solid sample): 3200 (w), 3083 (w), 2053 (m, C≡O), 1984 (m, C≡O), 1675 (s, C=O, TFA), 1435 (m), 1410 (m), 1395 (m), 1185 (s), 1131 (s), 842 (m), 797 (m), 724 (m). IR (solution): 2064 (symmetric $\nu_{C\equiv O}$), 1998 (antisymmetric $\nu_{C\equiv O}$). HR-ESI-MS (MeCN) $C_{21}H_{17}O_3NReRu$ $[M]^+$: calculated, 619.97930; found, 619.98032.

$[(Re(\eta^6\text{-}C_6H_6)(\eta^6\text{-}o\text{-}C_6H_4C(CH_3)(O)(C_5H_4N)Ru(CO)_2))_2]^{2+}$ ($[(\mathbf{4a})_2]^{2+}$ and $[(\mathbf{4b})_2]^{2+}$)

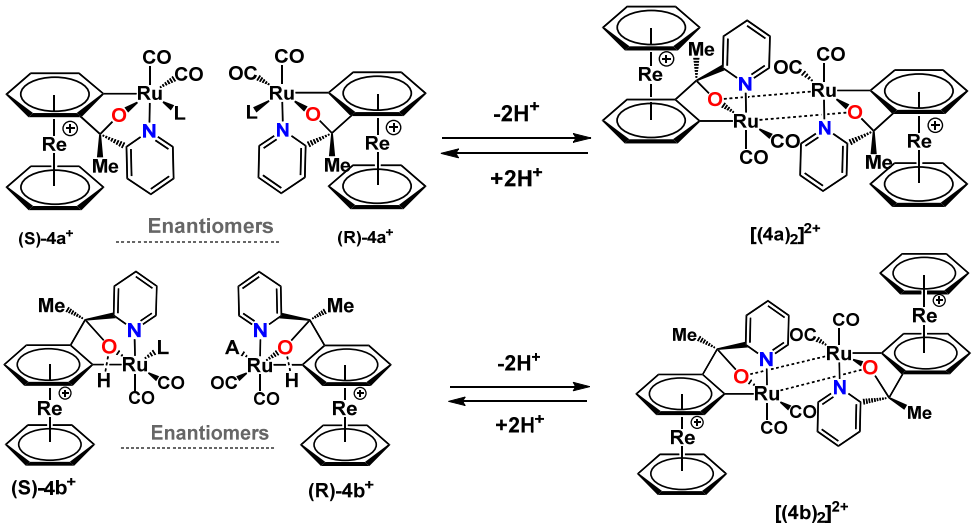

Synthesis: Complexes (±)-**4a**$^+$ and (±)-**4b**$^+$ spontaneously dimerize during work up if the pH conditions are slightly basic or neutral. In the particular case of complexes **$[(\mathbf{4a})_2]^{2+}$** and **$[(\mathbf{4b})_2]^{2+}$**, they were obtained after precipitation with NH_4PF_6 from a concentrated aqueous solution and subsequent intense washing with water. Work up can lead to the partial formation of dimers and thus a monomer-dimer mixture is obtained sometimes.

Analysis: $[(Re(\eta^6\text{-}C_6H_6)(\eta^6\text{-}o\text{-}C_6H_4C(CH_3)(O)(C_5H_4N)Ru(CO)_2))_2](PF_6)2$ **$[(\mathbf{4a})_2](PF_6)_2$**: ^{1}H NMR ($CD_3CN$, 500 MHz): 8.2 (dm, 1H, C*H*$_{pyridine}$), 8.24 (td, 1H, C*H*$_{pyridine}$), 7.83 (dt, 1H, C*H*$_{pyridine}$), 7.61 (ddd, 1H, C*H*$_{pyridine}$), 6.27 (d, 1H, C*H*$_{arene}$), 5.78 (d, 1H, C*H*$_{arene}$), 5.75 (t, 1H, C*H*$_{arene}$), 5.47 (t, 1H, C*H*$_{arene}$), 5.01 (s, 6H, C*H*$_{pyridine}$), 2.02 (s, 3H, C*H*$_3$); ^{13}C NMR (CD_3CN, 125 MHz): 197.85 (*C*O), 197.19 (*C*O), 168.55 (*C*$_{pyridine}$), 152.39 (*C*H$_{pyridine}$), 142.21 (*C*H$_{pyridine}$), 125.98 (*C*H$_{pyridine}$), 123.02 (*C*H$_{pyridine}$), 117.48 (*C*$_{arene}$), 110.55 (*C*$_{arene}$), 90.28 (*C*), 84.43 (*C*H$_{arene}$), 76.18 (*C*H$_{arene}$, according to ^{13}C HSQC two carbons have this chemical shift), 75.55 (*C*H$_{arene}$), 74.25 (*C*H$_{arene}$), 22.25 (*C*H$_3$). IR (solution, ACN): 2040 (symmetric $\nu_{C\equiv O}$), 1971 (antisymmetric $\nu_{C\equiv O}$). HR-ESI-MS (MeCN): $C_{42}H_{34}O_6N_2Re_2Ru_2$; $[M]^{2+}$; calculated, 619.98050; found, 619.98083.

$[(Re(\eta^6\text{-}C_6H_6)(\eta^6\text{-}o\text{-}C_6H_4C(CH_3)(O)(C_5H_4N)Ru(CO)_2))_2](PF_6)_2$ **$[(\mathbf{4b})_2](PF_6)_2$**: ^{1}H NMR ($CD_3CN$, 500 MHz): 8.98 (d, 1H, C*H*$_{pyridine}$), 8.18 (td, 1H, C*H*$_{pyridine}$), 7.96 (d, 1H, C*H*$_{pyridine}$), 7.68 (t, 1H, C*H*$_{pyridine}$), 6.05 (d, 1H, C*H*$_{arene}$), 5.89 (d, 1H, C*H*$_{arene}$), 5.64 (s, 6H, C*H*$_{arene}$), 5.61 (t, 1H, C*H*$_{arene}$), 5.56 (t, 1H, C*H*$_{pyridine}$), 1.90 (s, 3H, C*H*$_3$); ^{13}C NMR (CD_3CN, 125 MHz): 198.69 (*C*O), 198.30 (*C*O), 165.80 (*C*$_{pyridine}$), 152.89 (*C*H$_{pyridine}$), 142.47 (*C*H$_{pyridine}$), 126.35 (*C*H$_{pyridine}$), 123.74 (*C*H$_{pyridine}$), 121.24 (*C*$_{arene}$), 108.54 (*C*$_{arene}$), 90.62 (*C*), 87.29 (*C*H$_{arene}$), 76.58 (*C*H$_{arene}$), 76.09 (*C*H$_{arene}$), 75.86 (*C*H$_{arene}$), 74.53 (*C*H$_{arene}$), 21.60 (*C*H$_3$). IR (solution, ACN): 2034 (symmetric $\nu_{C\equiv O}$), 1968 (antisymmetric $\nu_{C\equiv O}$). HR-ESI-MS (MeCN): $C_{42}H_{34}O_6N_2Re_2Ru_2$; $[M]^{2+}$; calculated, 619.98040; found, 619.98070.

UPLC-MS chromatograms

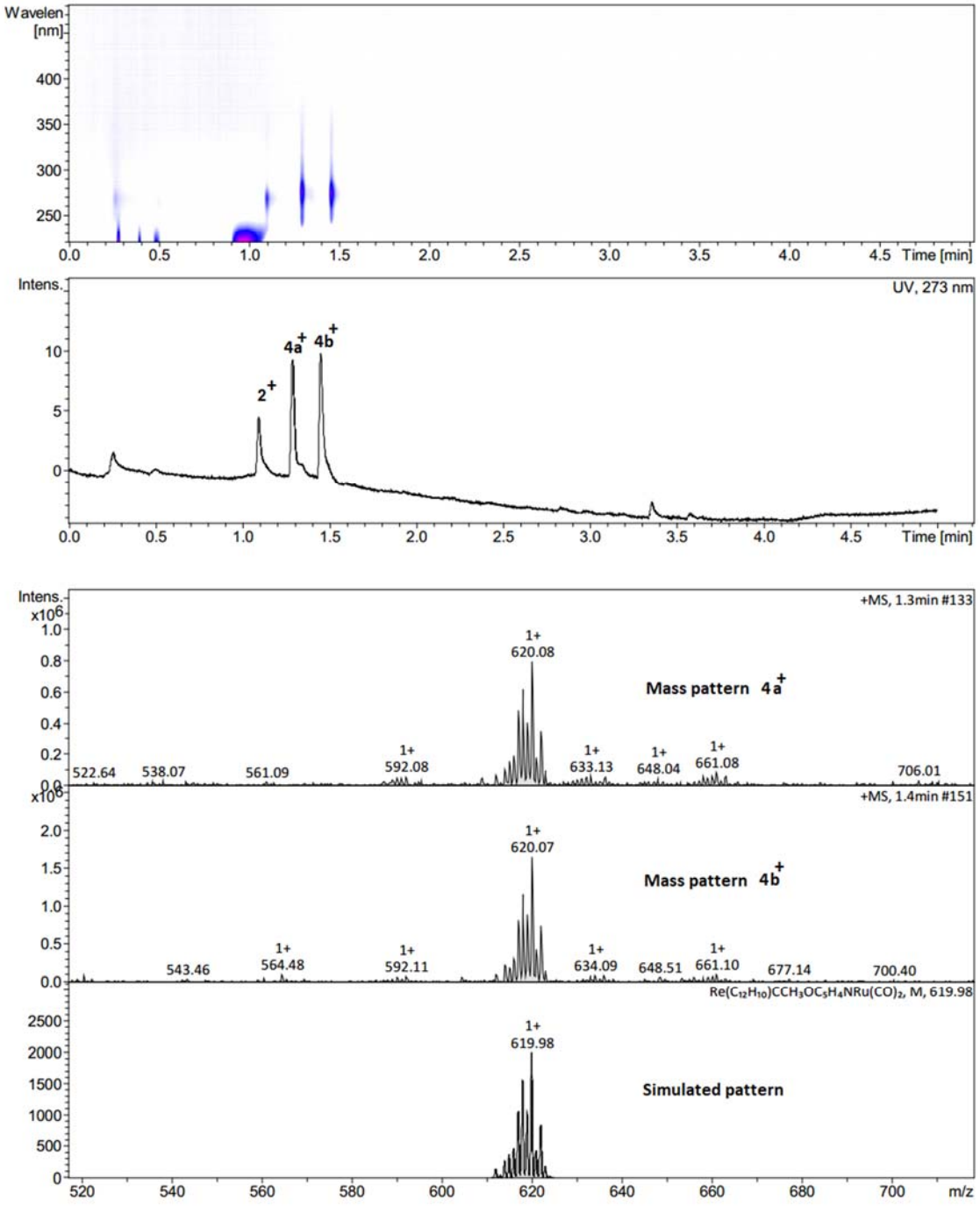

Figure S1. Reaction control after 70 min. UV trace (top) and MS (bottom).

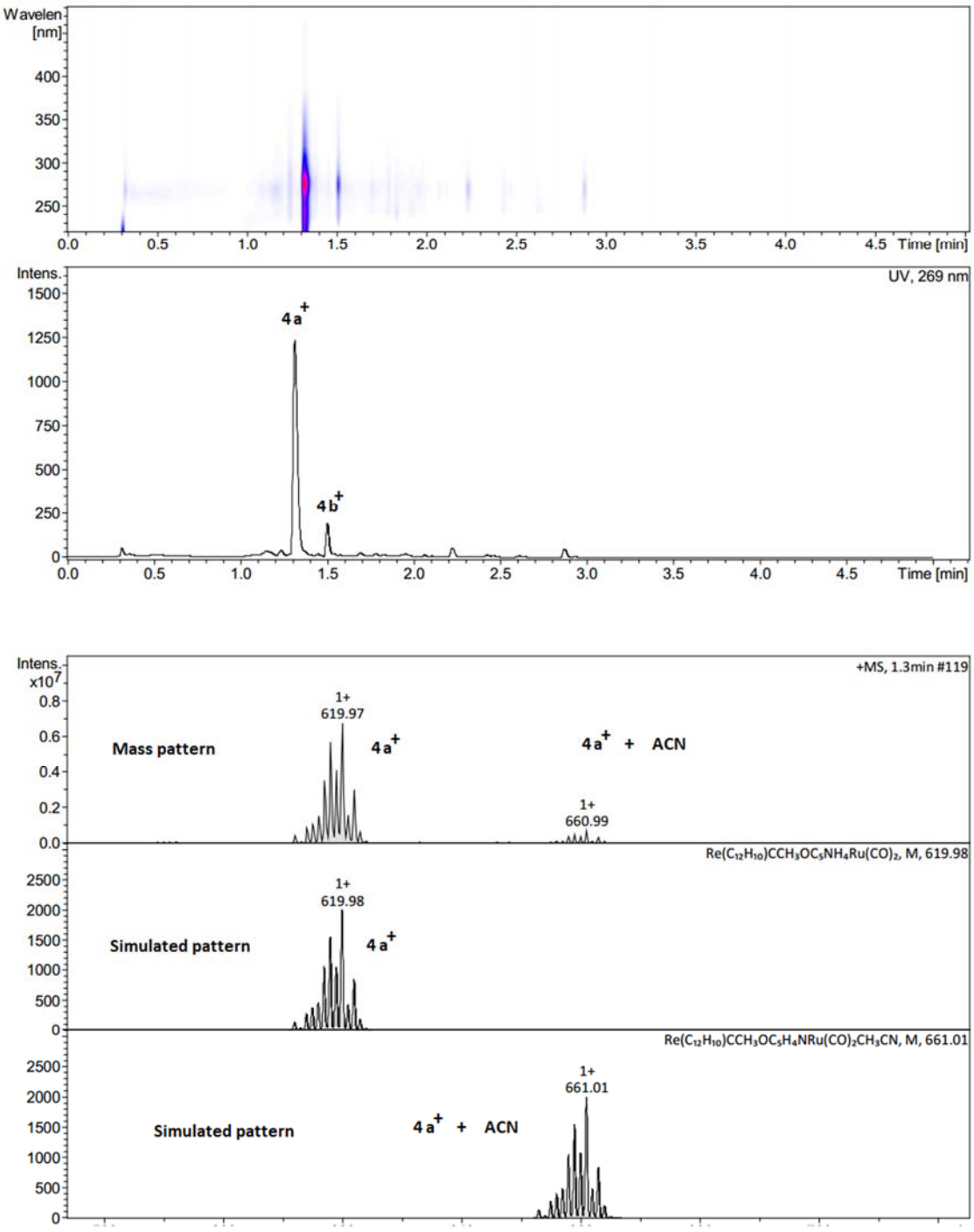

Figure S2. Experimental and simulated mass pattern for (±)-**4a**$^{+}$. The sixth coordination site is occupied by acetonitrile.

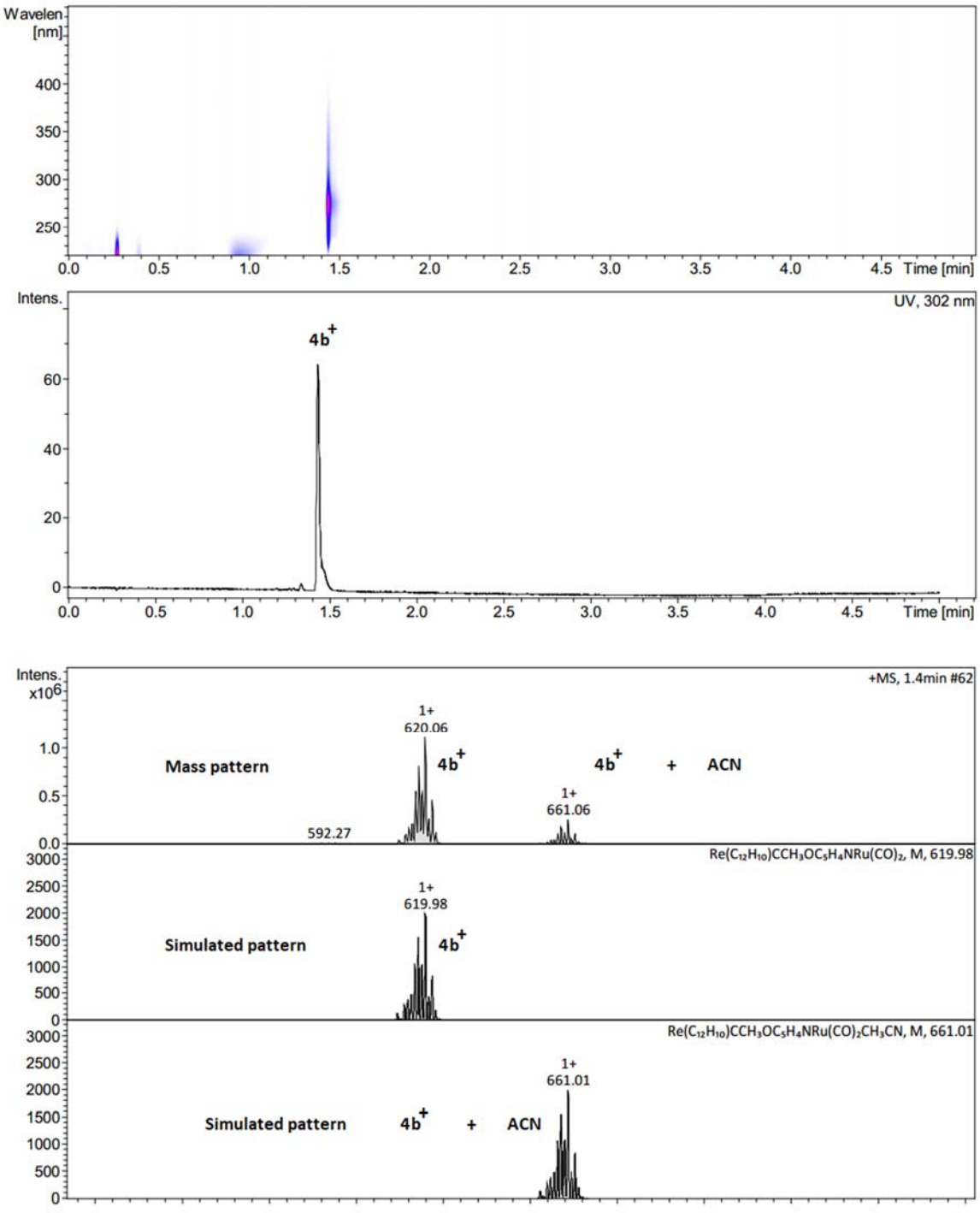

Figure S3. Experimental and simulated mass pattern for (±)-**4b**$^{+}$. The sixth coordination site is occupied by acetonitrile.

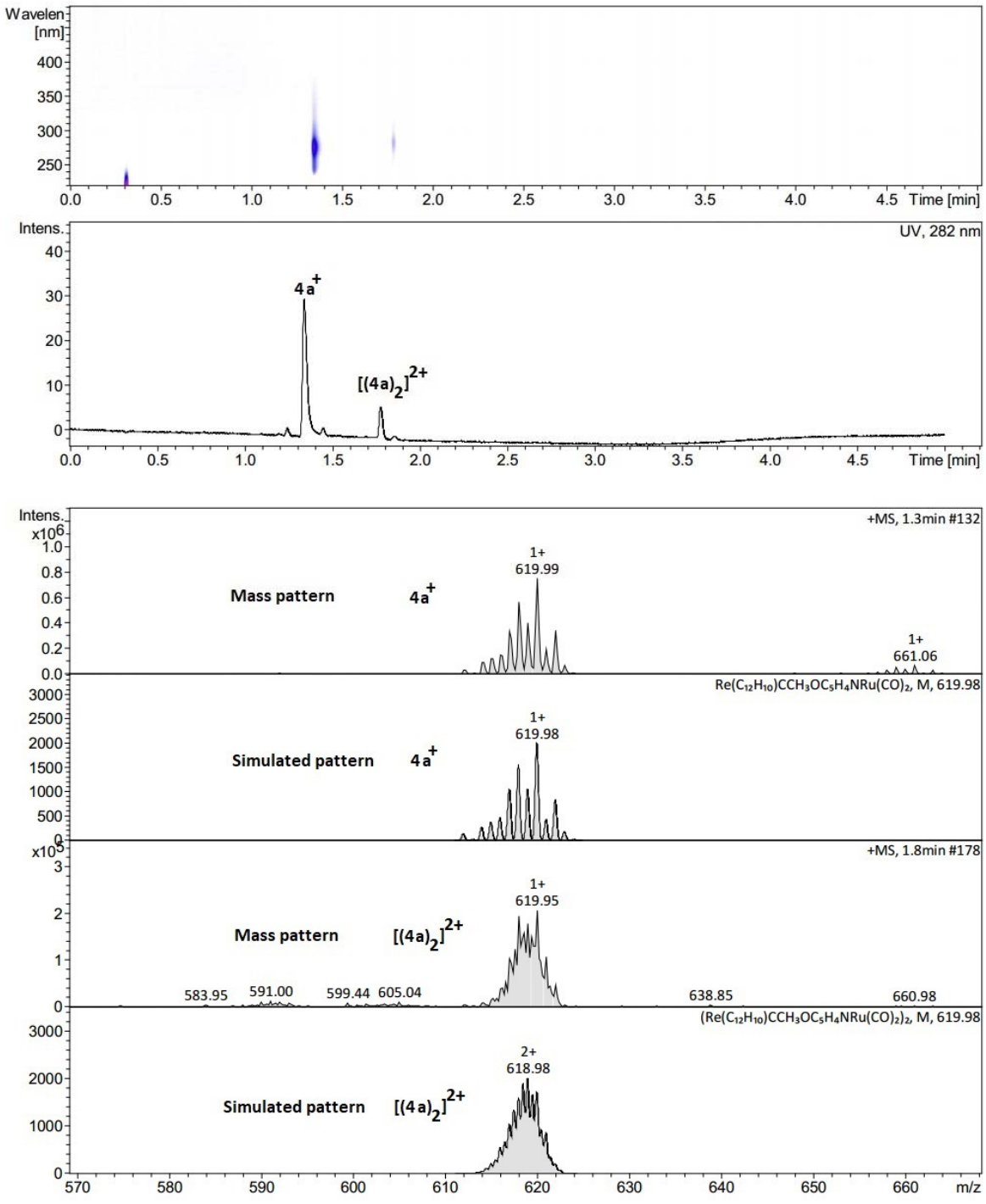

Figure S4. Experimental and simulated mass pattern for **$[(4a)_2]^{2+}$**. Comparison with **$4a^+$**.

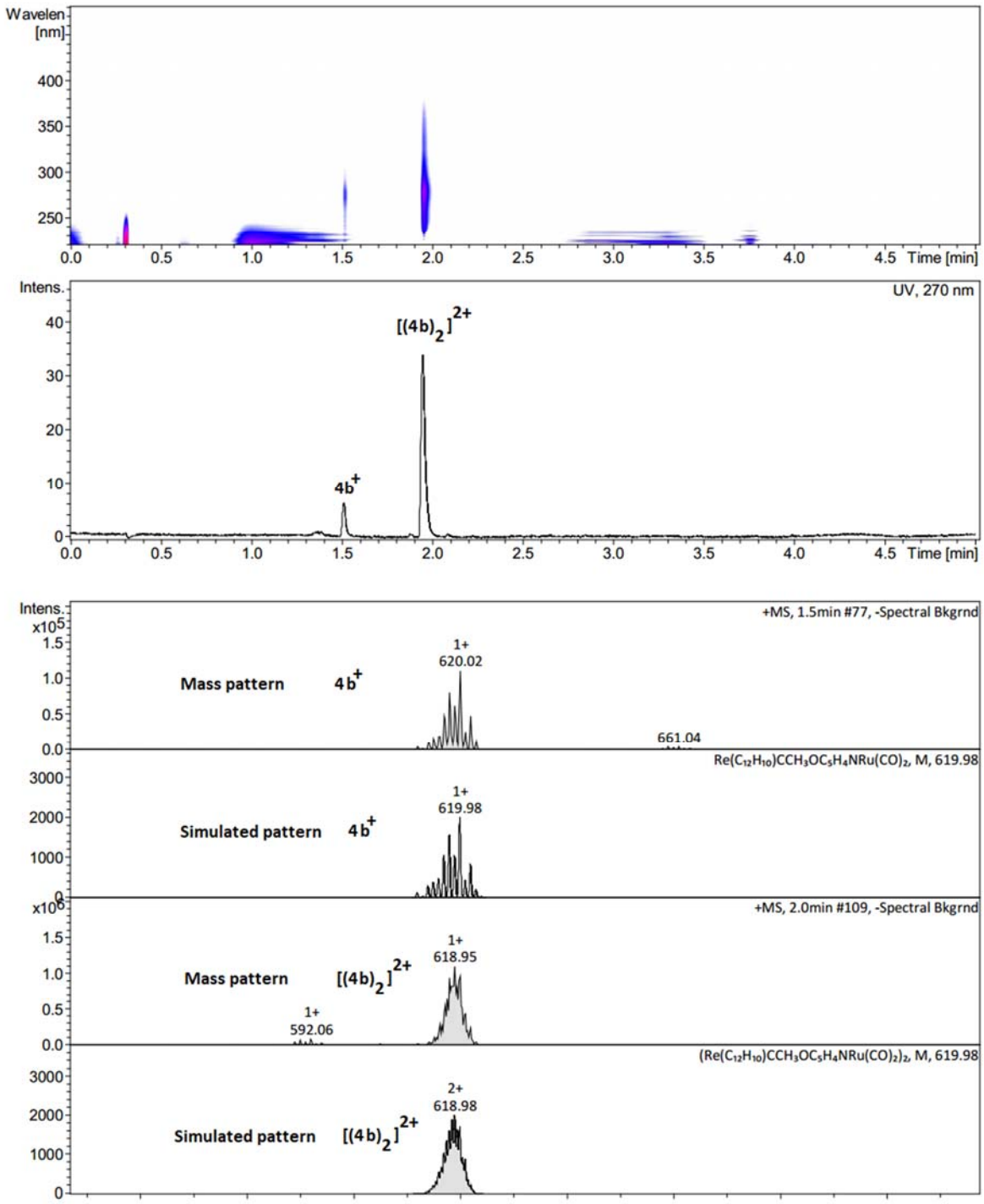

Figure S5. Experimental and simulated mass pattern for **$[(4a)_2]^{2+}$**. Comparison with **$4a^+$**.

3. HR-ESI-MS

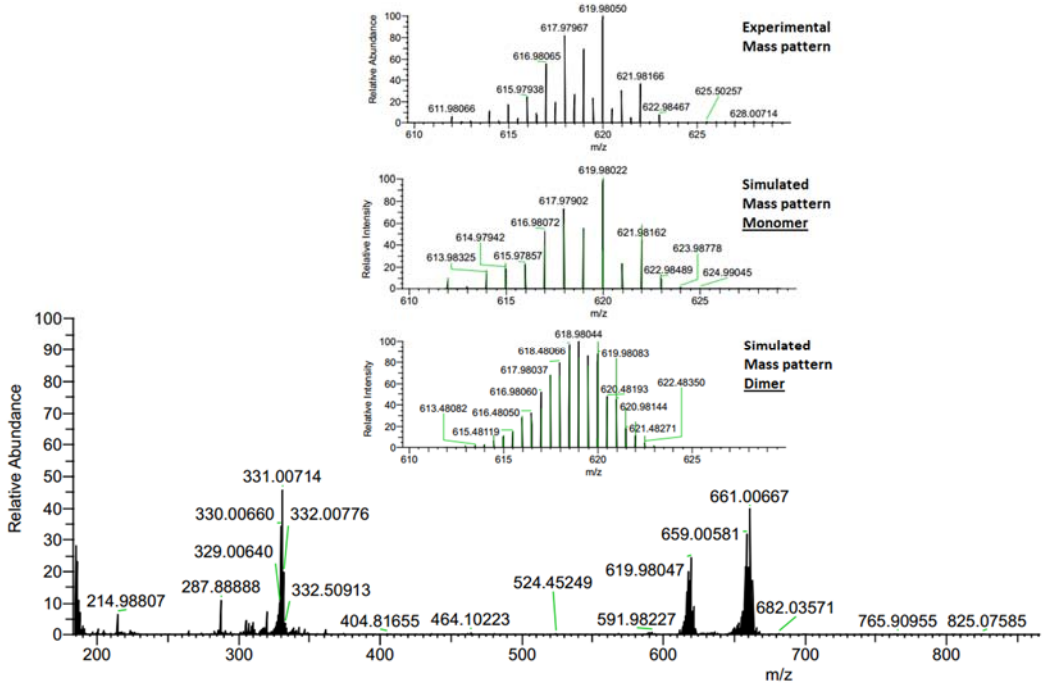

Figure S6. HR-ESI-MS for the mixture of complexes (±)-**4a**$^{+}$ and **[(4a)$_2$]**$^{2+}$ (monomer-dimer mixture). The simulated mass pattern confirms the presence of a dimer.

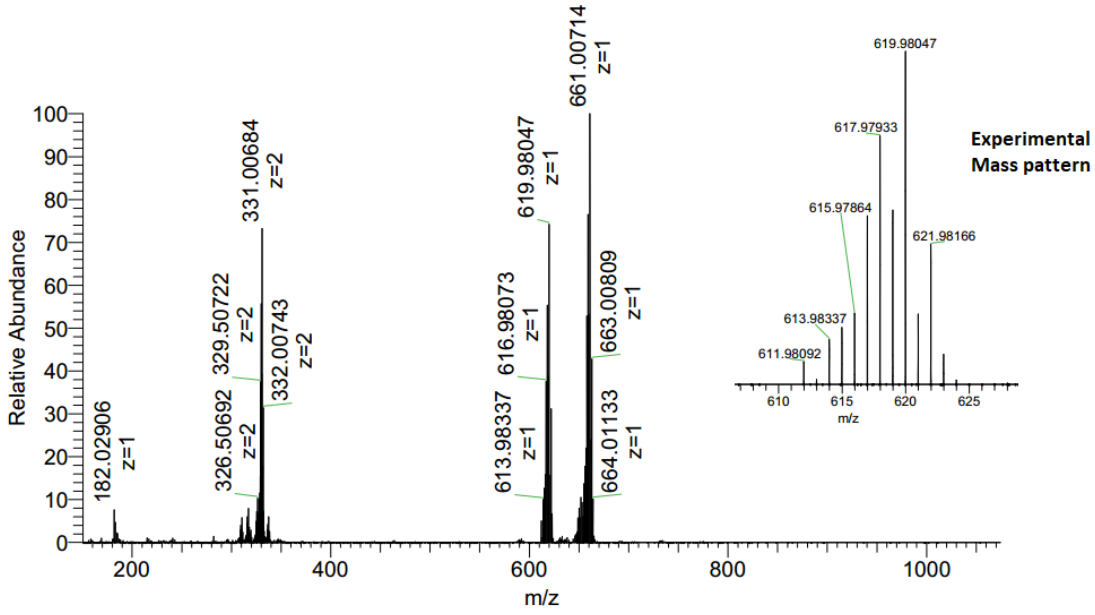

Figure S7. HR-ESI-MS for **4b**$^{+}$. The simulated mass pattern confirms the presence of a monomer. The m/z = 661.00714 confirms the ACN coordinated to Ru(II).

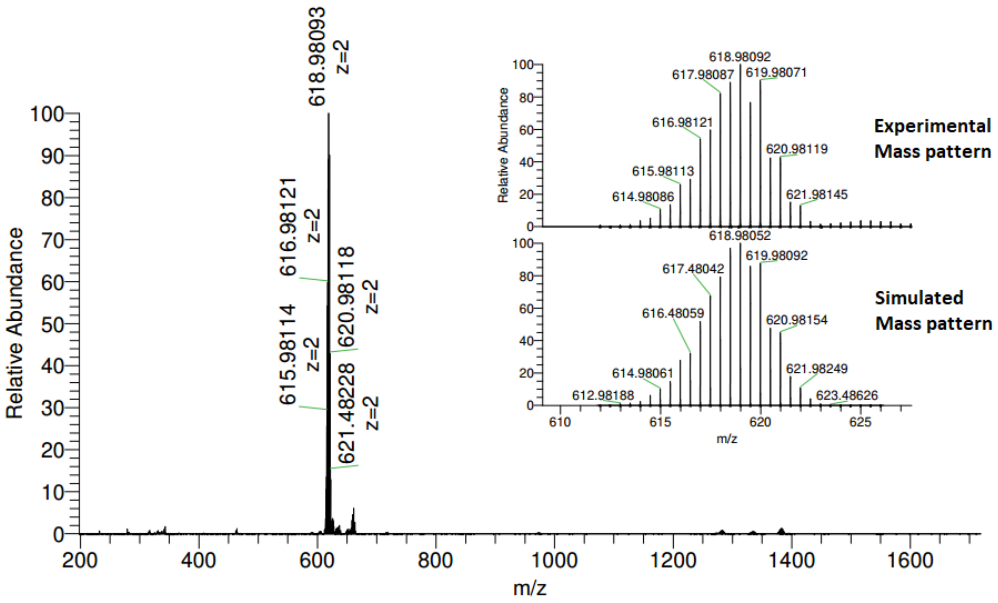

Figure S8. HR-ESI-MS for **[(4b)$_2$]$^{2+}$**. The simulated mass pattern confirms the presence of a dimer.

4. NMR spectra

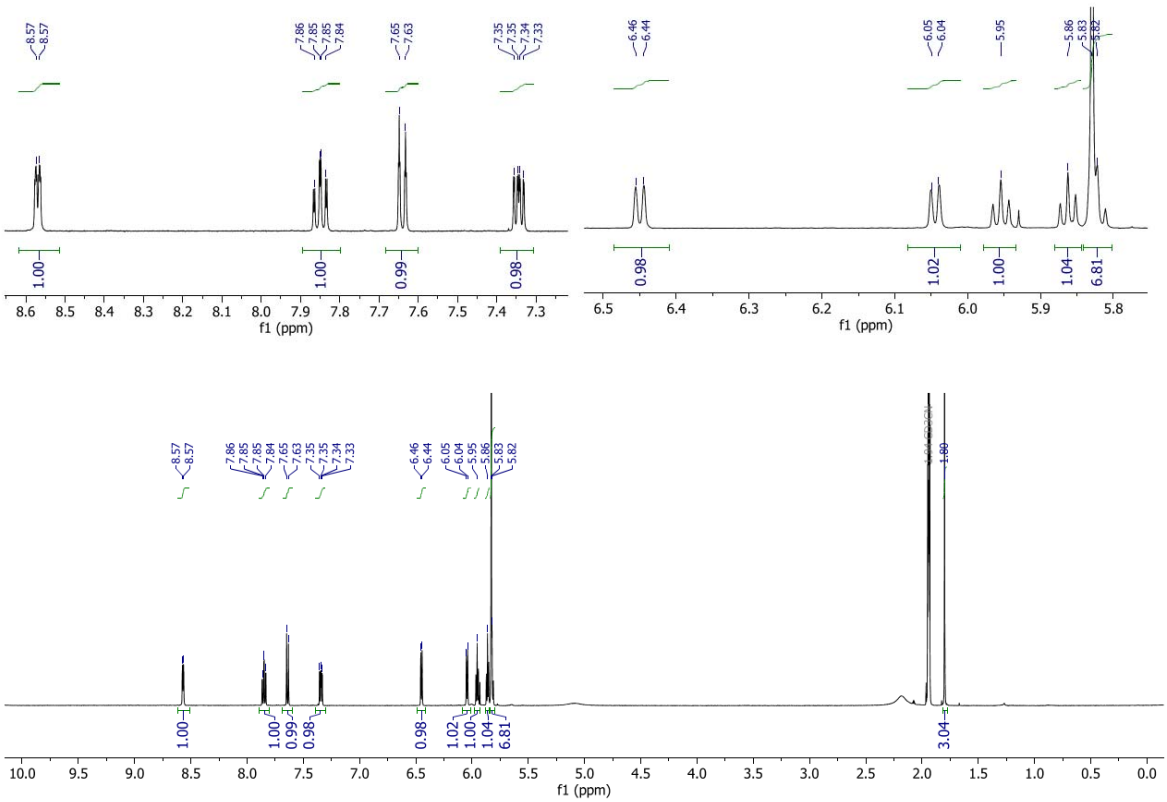

Figure S9. ^{1}H NMR of complex **2$^+$**. 500 MHz, CD_3CN, 295K

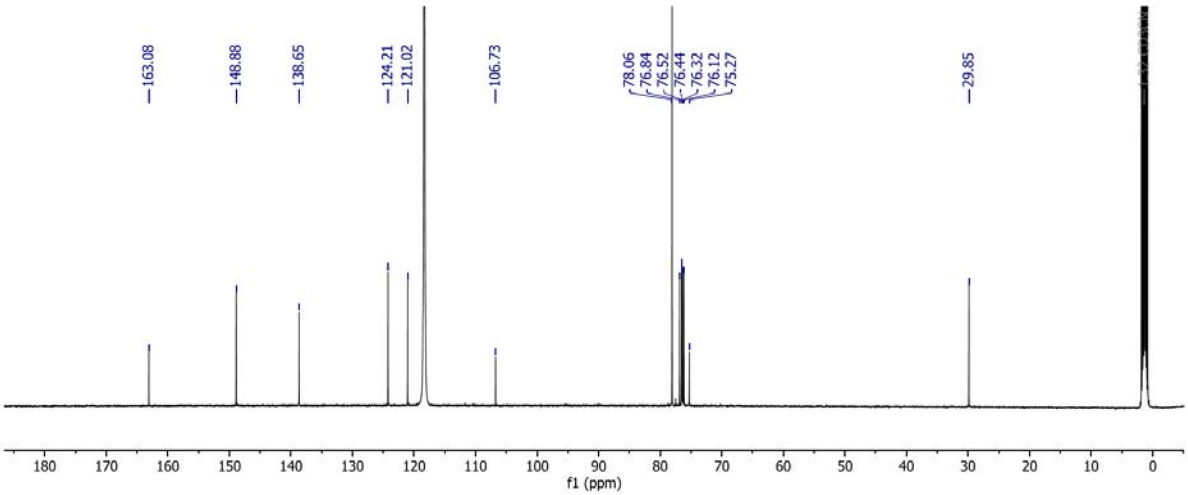

Figure S10. ^{13}C NMR of complex $\mathbf{2}^{+}$. 125 MHz, CD_3CN, 295K

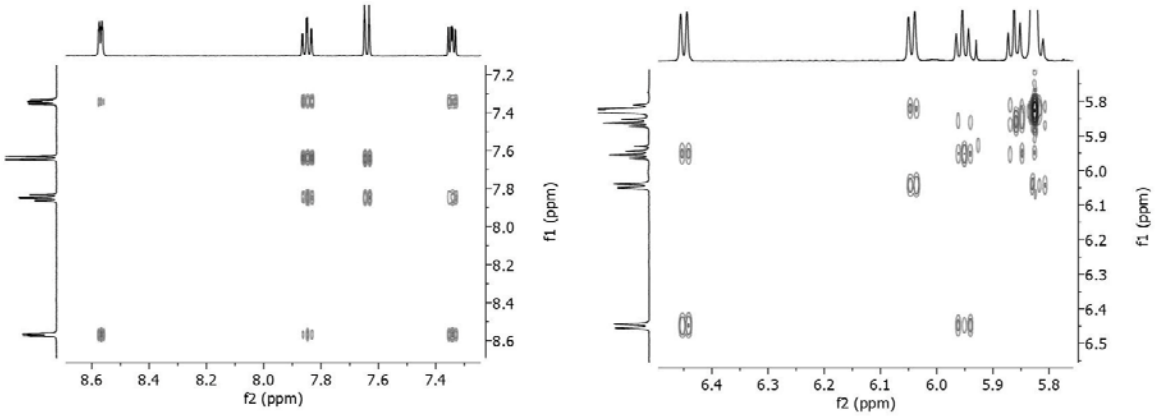

Figure S11. 2D-^{1}H COSY of complex $\mathbf{2}^{+}$. 500MHz, CD_3CN, 295K

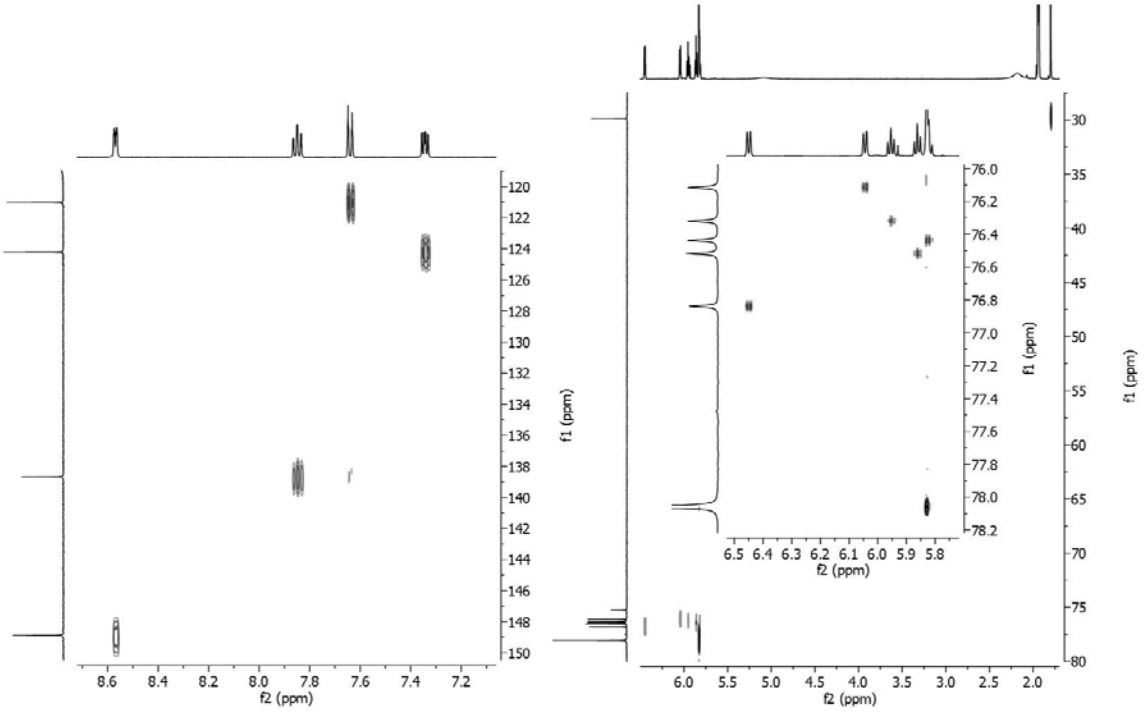

Figure S12. 2D-^{13}C HSQC of complex **2**$^{+}$. 500MHz, CD_3CN, 295K.

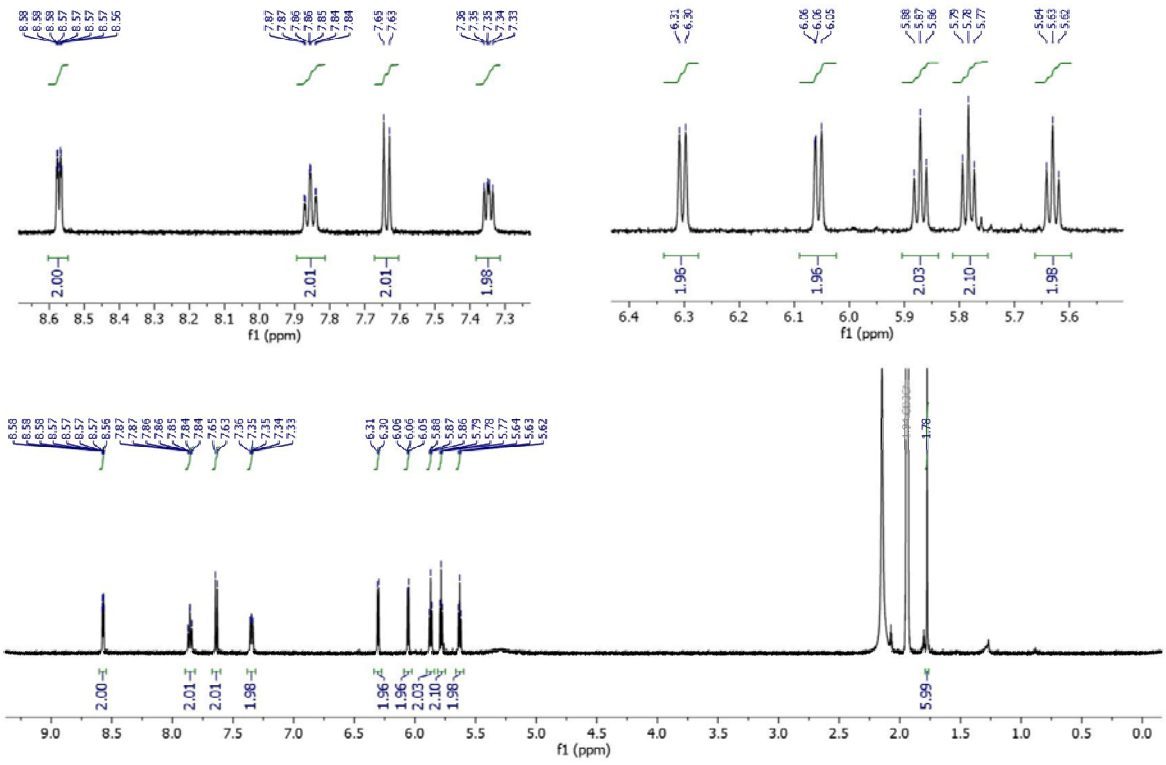

Figure S13. ^{1}H NMR of complex **3**$^{+}$. 500MHz, CD_3CN, 295K

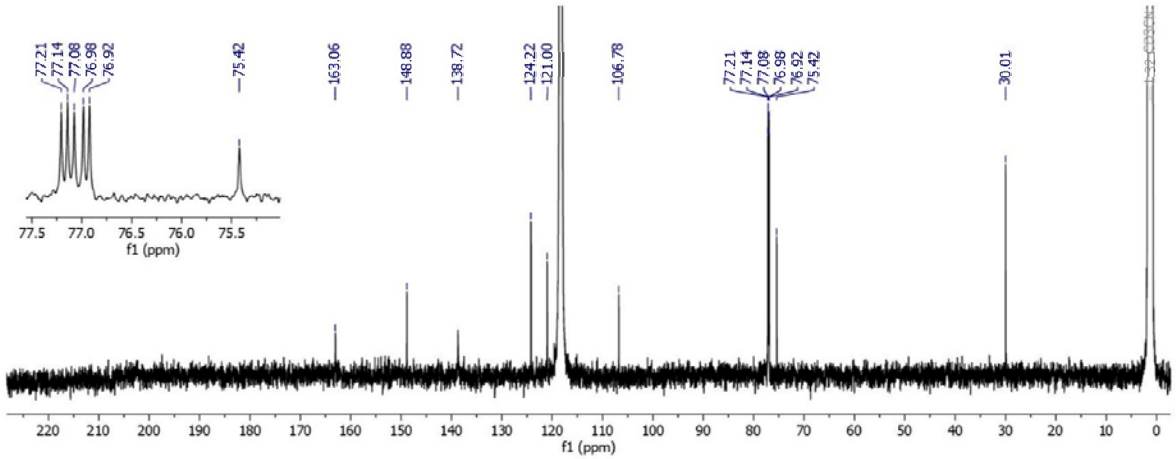

Figure S14. ^{13}C NMR of complex $\mathbf{3}^{+}$. 125MHz, CD_3CN, 295K

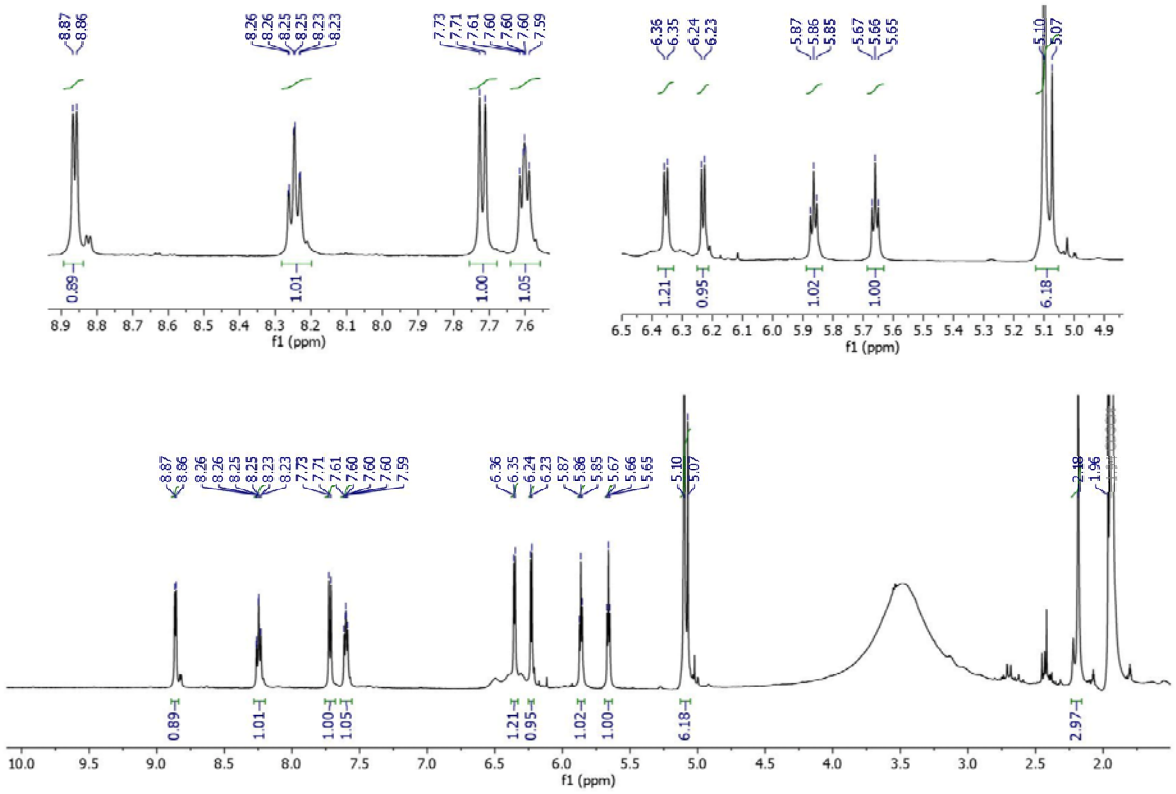

Figure S15. ^{1}H NMR of complex (±)-$\mathbf{4a}^{+}$. 500 MHz, CD_3CN, 295K

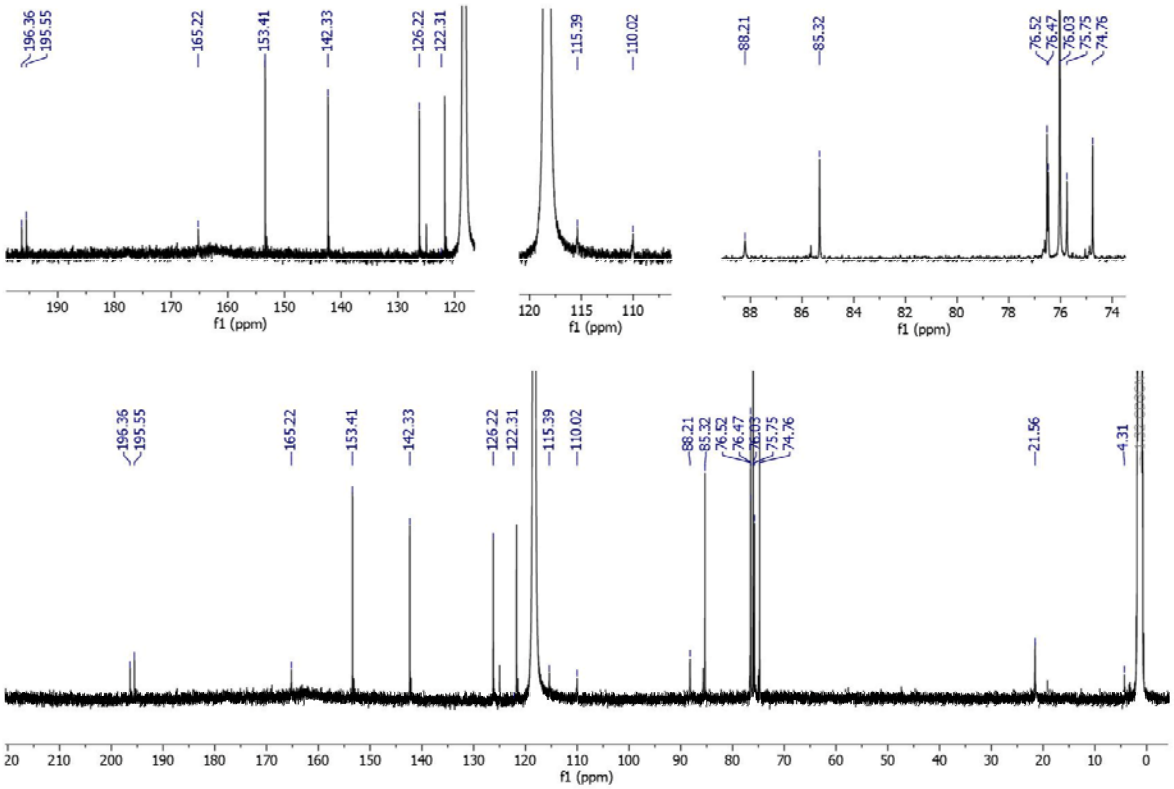

Figure S16. ^{13}C NMR of complex (±)-**4a**$^{+}$. 500 MHz, CD_3CN, 295K

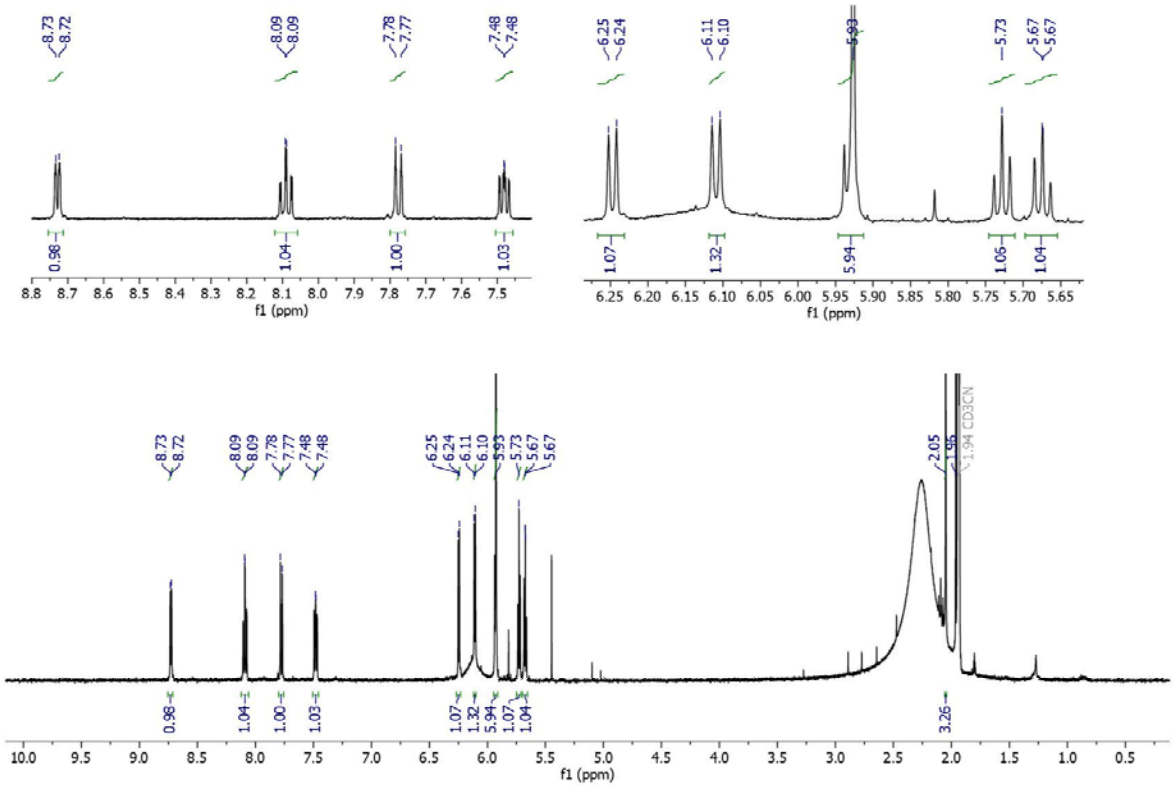

Figure S17. ^{1}H NMR of complex (±)-**4b**$^{+}$. 500 MHz, CD_3CN, 295K

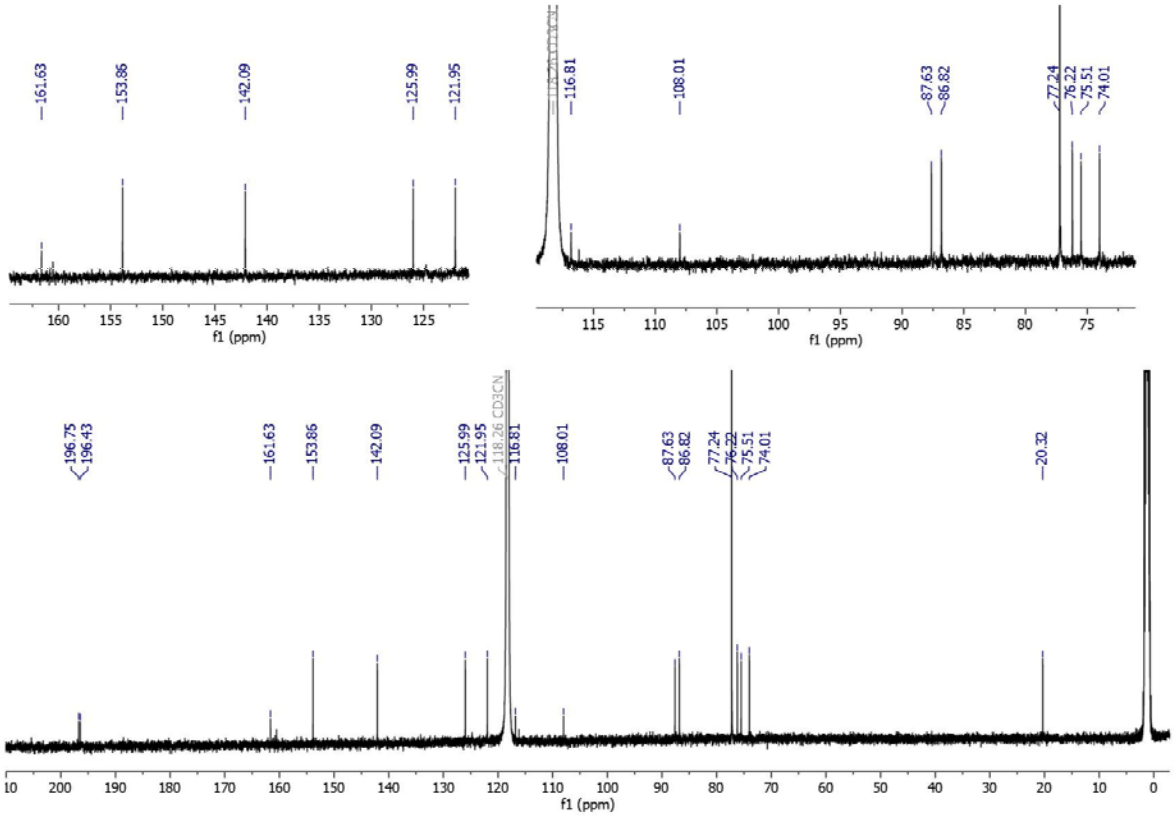

Figure S18. ^{13}C NMR of complex (±)-**4b**$^{+}$. 500 MHz, CD_3CN, 295K

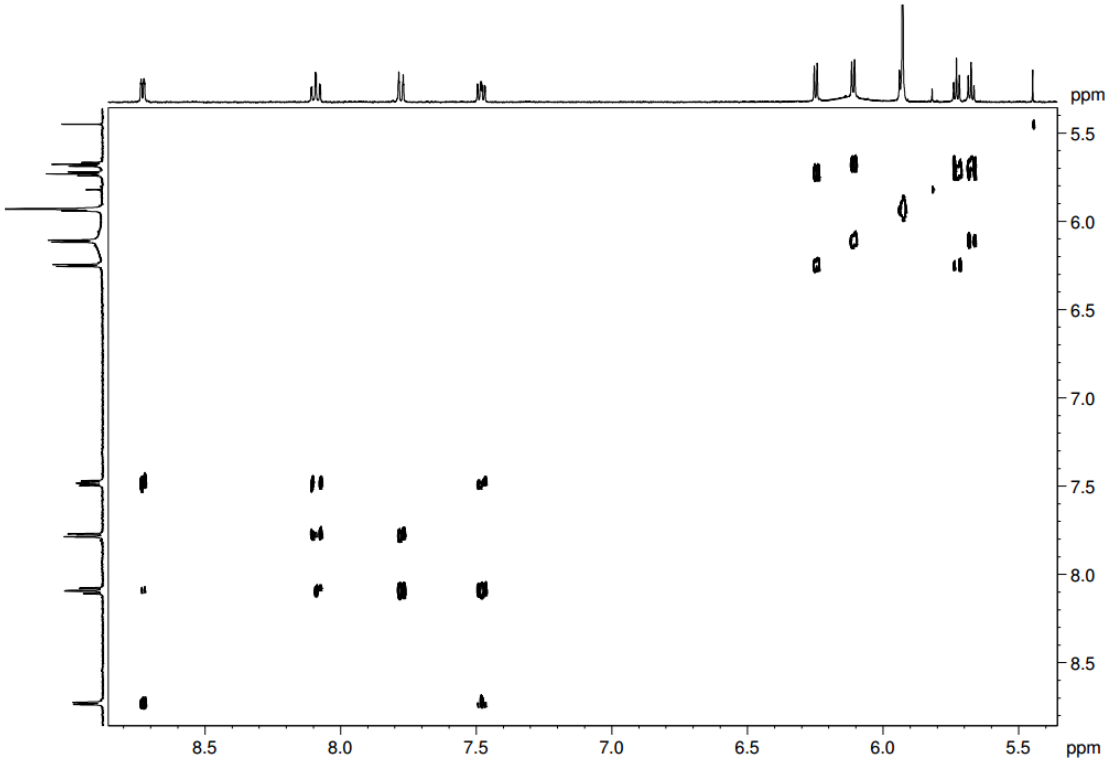

Figure S19. 2D-^{1}H COSY of complex (±)-**4b**$^{+}$. 500 MHz, CD_3CN, 295K

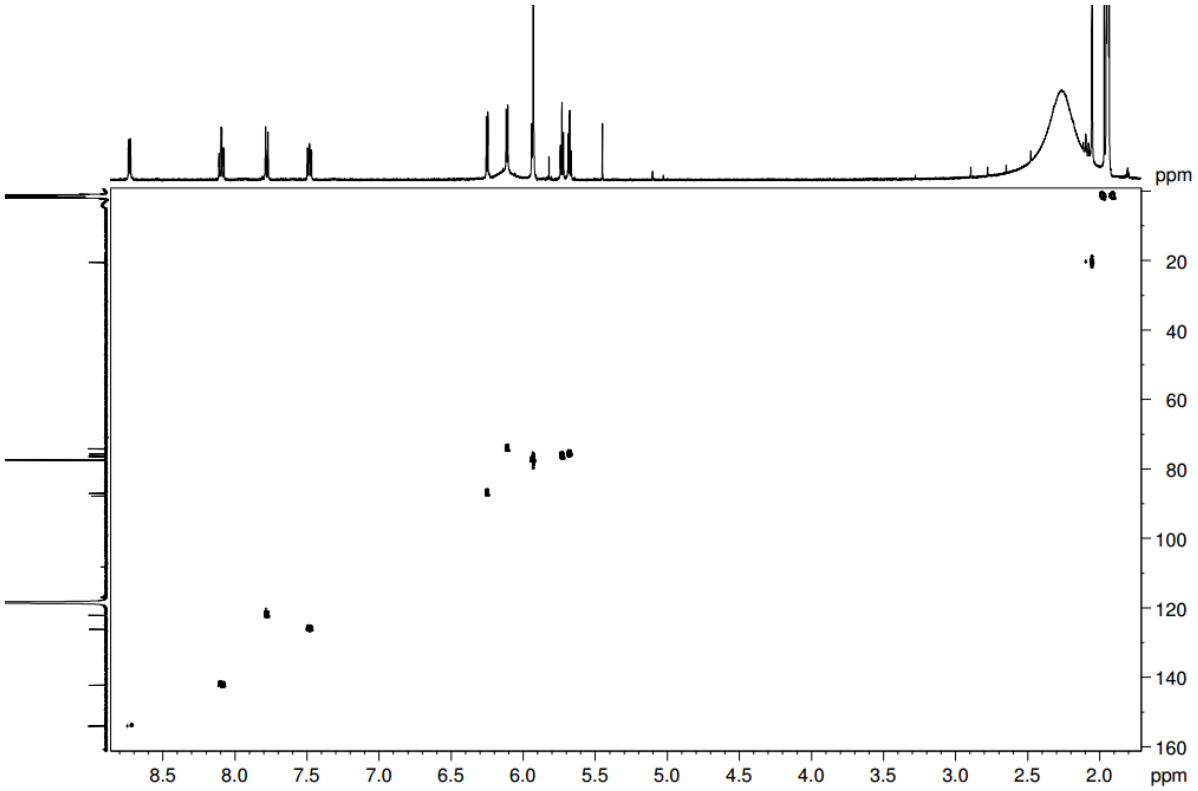

Figure S20. 2D-^{13}C HSQC of complex (±)-**4b**$^{+}$. 500 MHz, CD_3CN, 295K

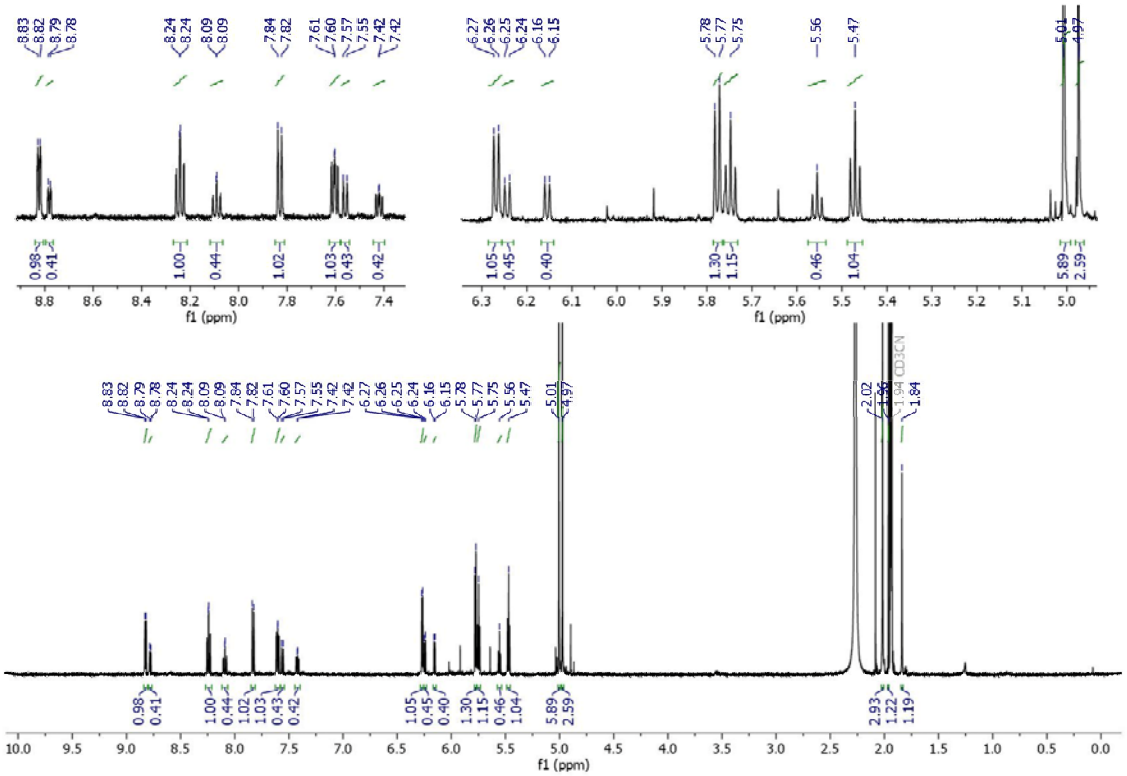

Figure S21. ^{1}H NMR of a mixture (30:70) of complex (±)-**4a**$^{+}$ and its dimer **[(4a)$_2$]**$^{2+}$. 500MHz, CD_3CN, 295K.

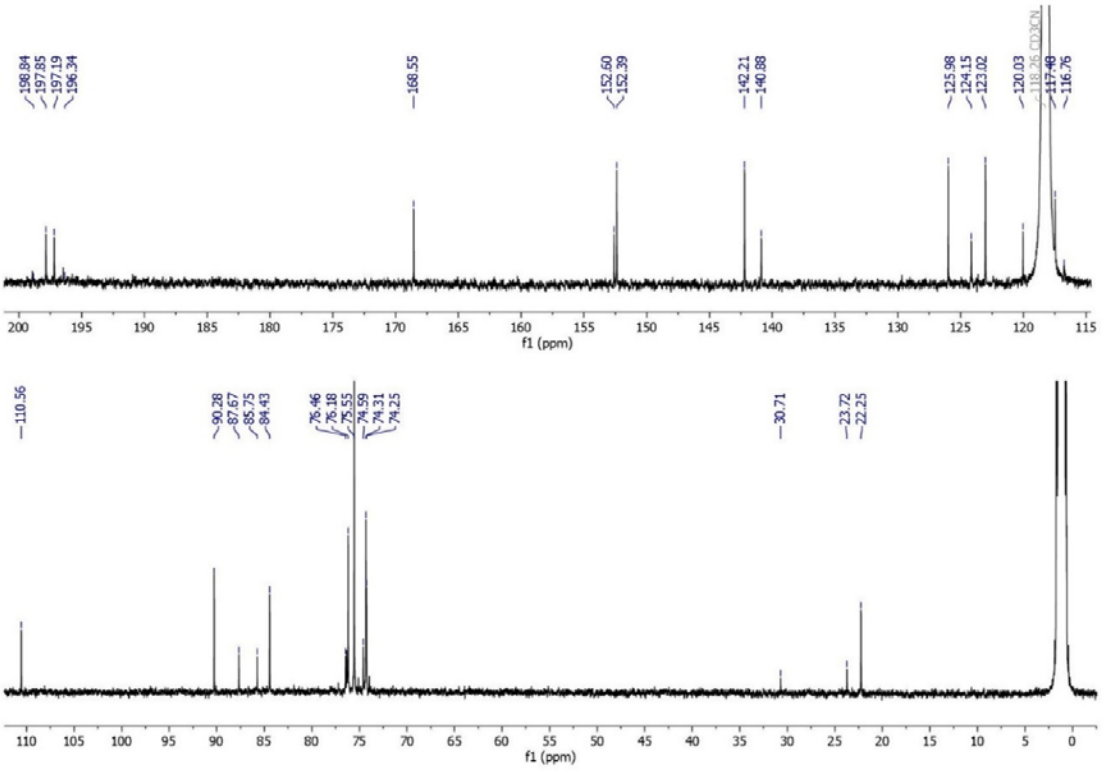

Figure S22. ^{13}C NMR of a mixture (30:70) of complex (±)-**4a**$^{+}$ and its dimer **[(4a)$_2$]**$^{2+}$. 125 MHz, CD_3CN, 295K.

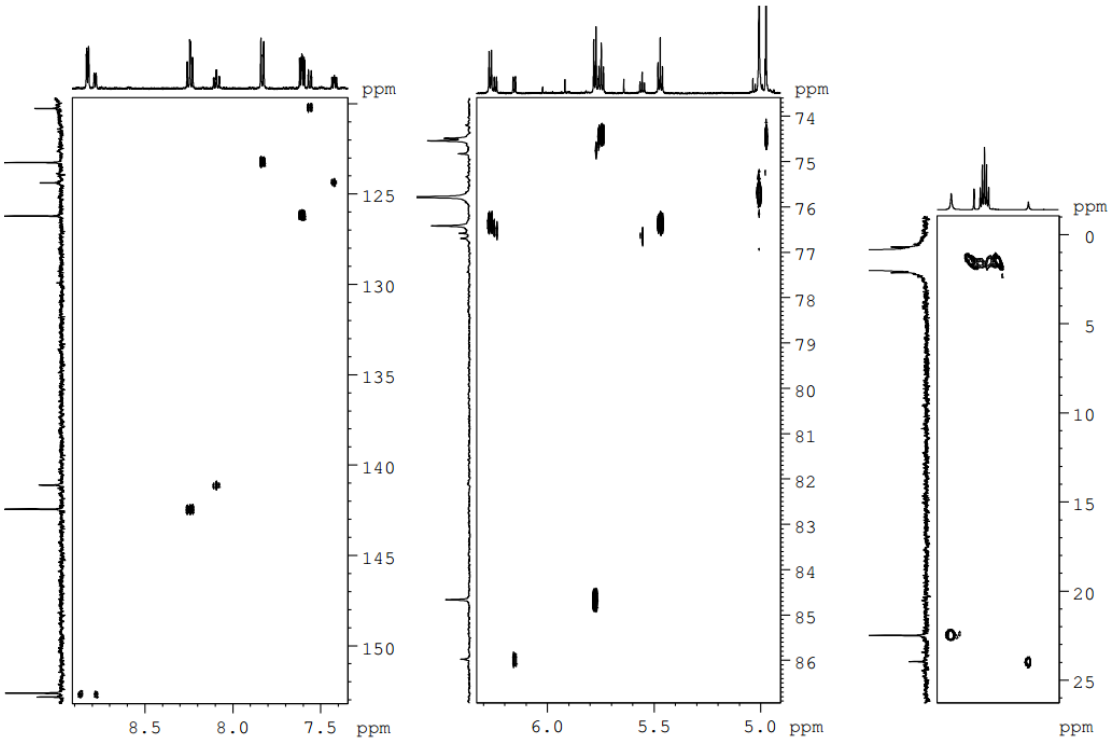

Figure S23. 2D-^{13}C HSQC of a mixture (30:70) of complex (±)-**4a**$^{+}$ and its dimer **[(4a)$_2$]**$^{2+}$. 500MHz, CD_3CN, 295K.

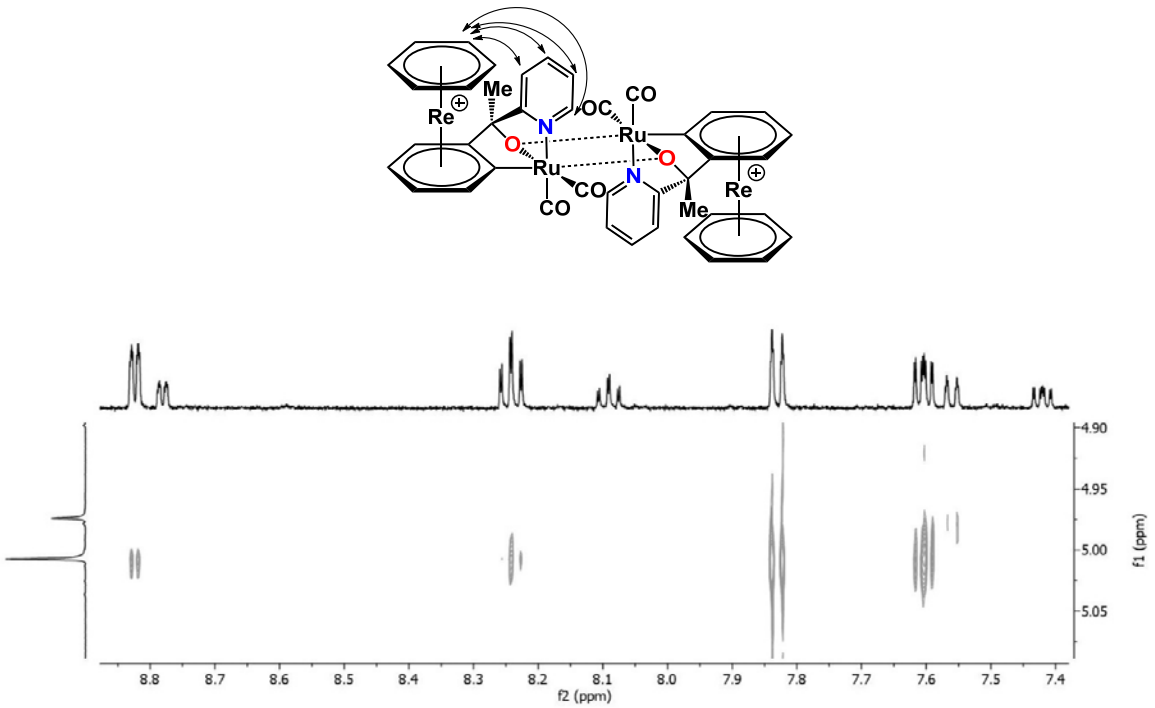

Figure S24. 2D-^{1}H ROESY of a mixture (30:70) of complex (±)-**4a**$^{+}$ and its dimer **[(4a)$_2$]**$^{2+}$. 500MHz, CD_3CN, 295K.

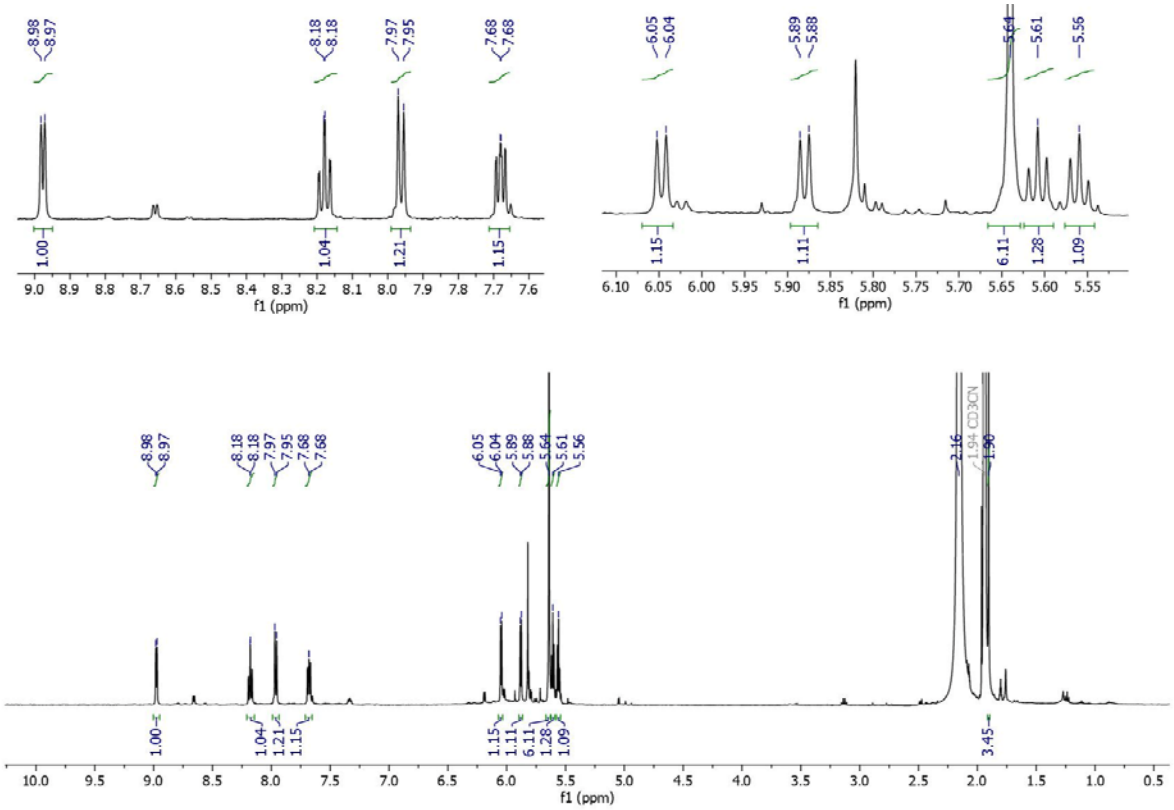

Figure S25. ^{1}H NMR of complex **[(4b)$_2$]**$^{2+}$. 500 MHz, CD_3CN, 295K

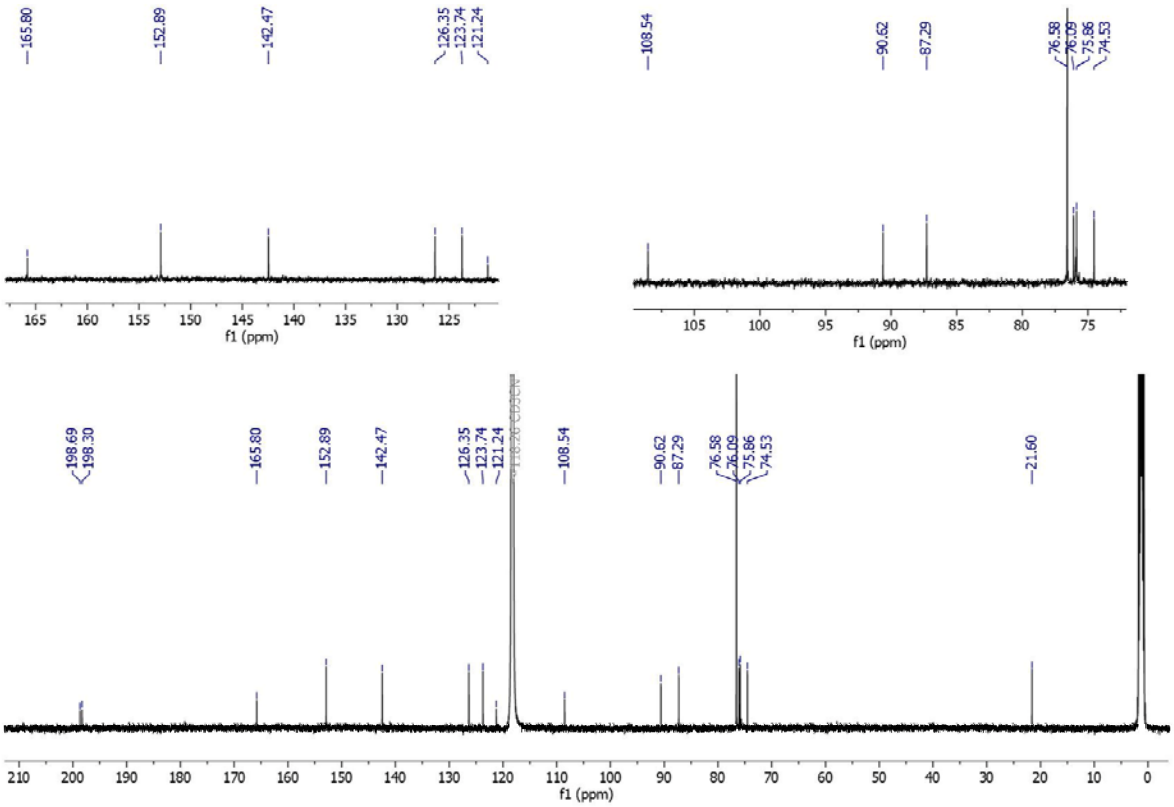

Figure S26. ^{13}C NMR of complex $[(\mathbf{4b})_2]^{2+}$. 500 MHz, CD_3CN, 295K

5. Kinetics

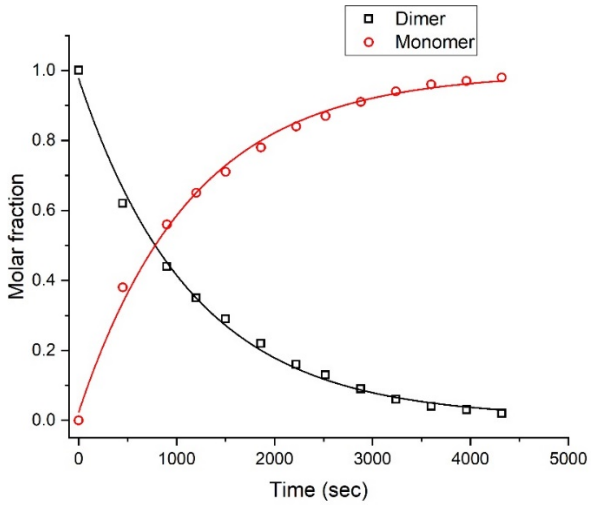

Figure S27. Kinetic data for the dimer splitting after addition of 111 mM of HTFA. Intial concentration of $[(\mathbf{4b})_2]^{2+}$ is 1.11 mM. The plot shows the peak integral corresponding to the 6 chemically equivalent arene protons (δ_{dimer} = 5.64, $\delta_{monomer}$ = 5.93) in CD_3CN.

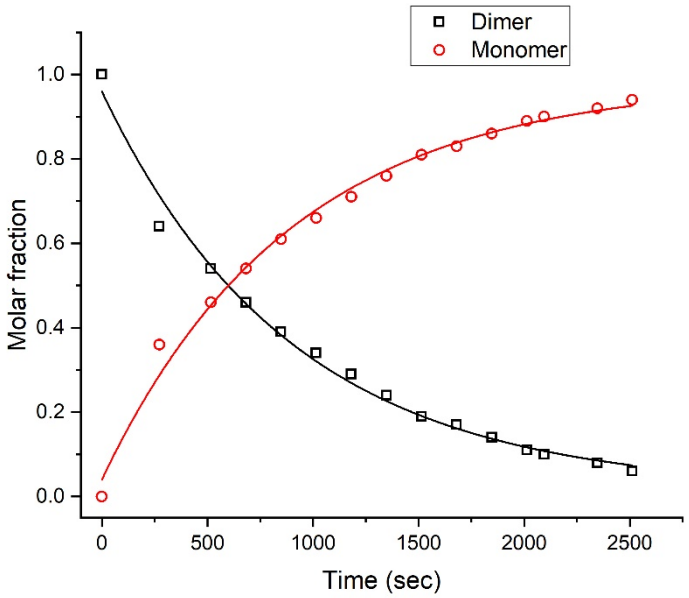

Figure S28. Kinetic data for the dimer splitting after addition of 138 mM of HTFA. Intial concentration of **[(4b)$_2$]$^{2+}$** is 1.11 mM. The plot shows the peak integral corresponding to the 6 chemically equivalent arene protons (δ_{dimer} = 5.64, $\delta_{monomer}$ = 5.93) in CD_3CN.

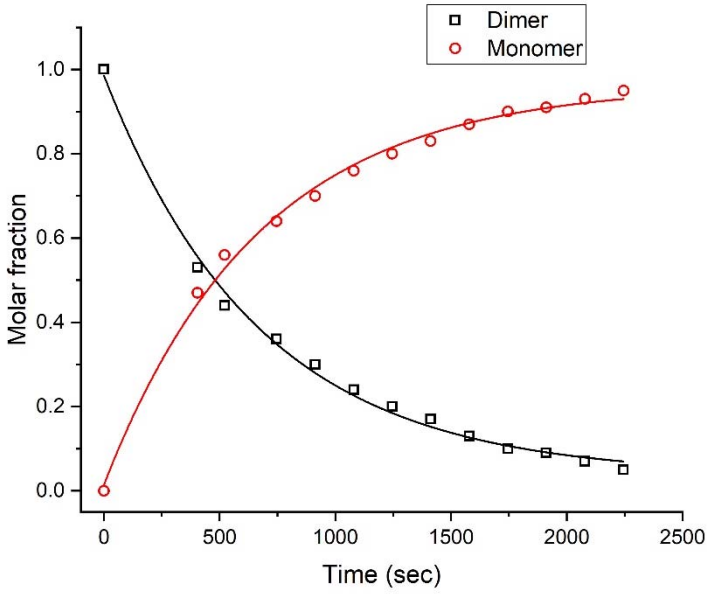

Figure S29. Kinetic data for the dimer splitting after addition of 166 mM of HTFA. Initial concentration of **[(4b)$_2$]$^{2+}$** is 1.11 mM. The plot shows the peak integral corresponding to the 6 chemically equivalent arene protons (δ_{dimer} = 5.64, $\delta_{monomer}$ = 5.93) in CD_3CN.

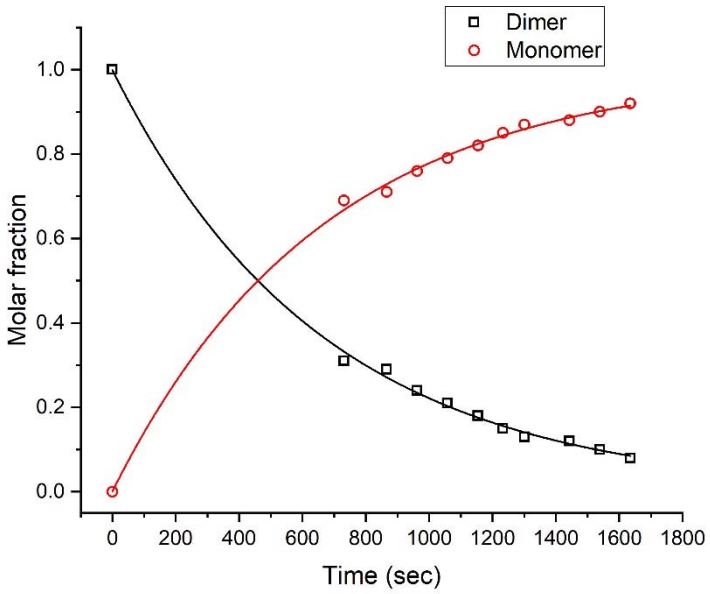

Figure S30. Kinetic data for the dimer splitting after addition of 179 mM of HTFA. Initial concentration of **$[(4b)_2]^{2+}$** is 1.11 mM. The plot shows the peak integral corresponding to the 6 chemically equivalent arene protons (δ_{dimer} = 5.64, $\delta_{monomer}$ = 5.93) in CD_3CN.

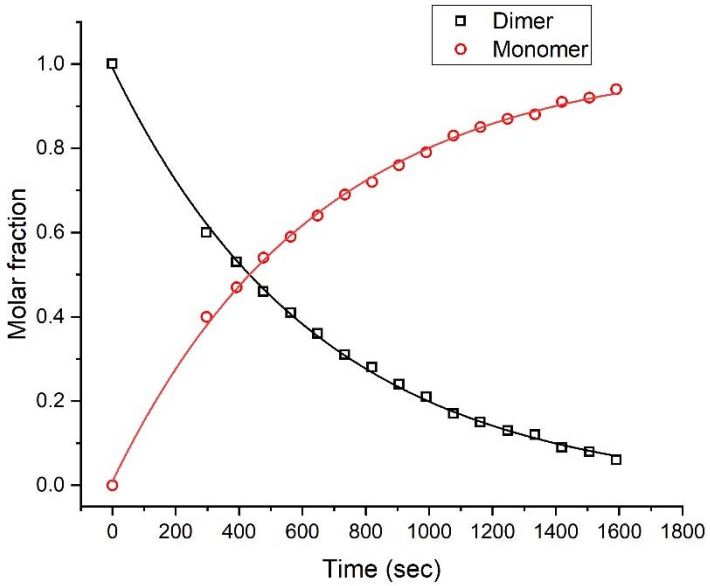

Figure S31. Kinetic data for the dimer splitting after addition of 193 mM of HTFA. Initial concentration of **$[(4b)_2]^{2+}$** is 1.11 mM. The plot shows the peak integral corresponding to the 6 chemically equivalent arene protons (δ_{dimer} = 5.64, $\delta_{monomer}$ = 5.93) in CD_3CN.

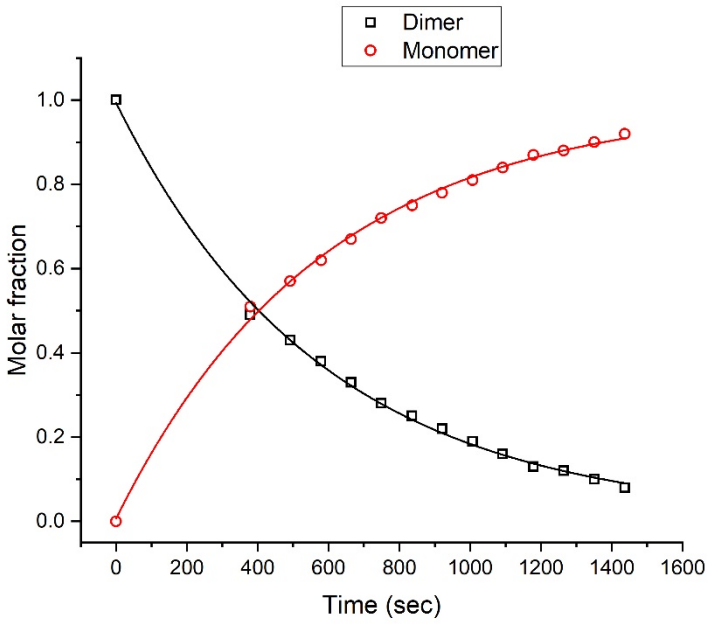

Figure S32. Kinetic data for the dimer splitting after addition of 207 mM of HTFA. Initial concentration of **$[(4b)_2]^{2+}$** is 1.11 mM. The plot shows the peak integral corresponding to the 6 chemically equivalent arene protons (δ_{dimer} = 5.64, $\delta_{monomer}$ = 5.93) in CD_3CN.

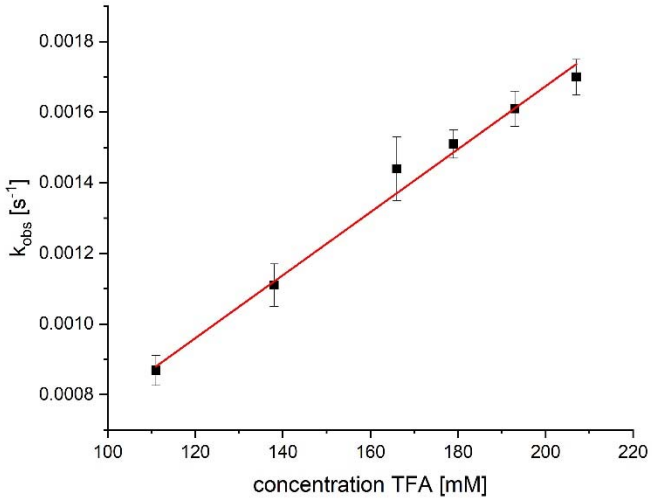

Figure S33. Representation of the observed rate constants k_{obs} vs concentration of HTFA. Linearization gives the 2nd order rate constant for the dimer splitting into monomers.

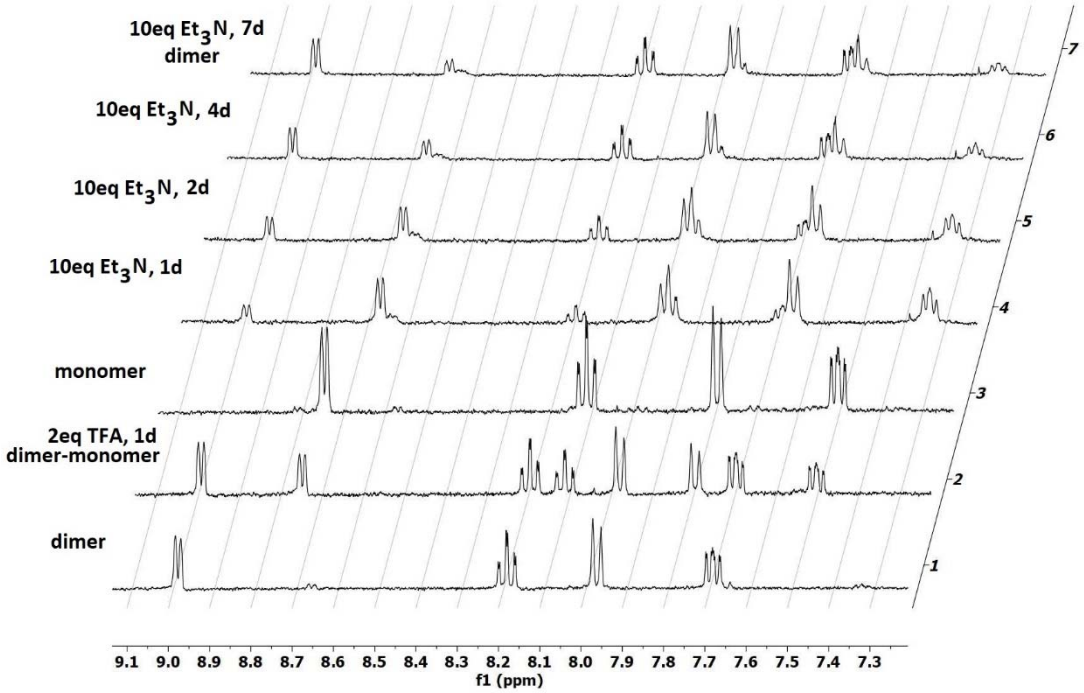

Figure S34. Waterfall plot of reversible dimer-monomer equilibrium after addition of HTFA and Et_3N. Initial concentration of $\mathbf{[(4b)_2]^{2+}}$ is 1.11 mM.

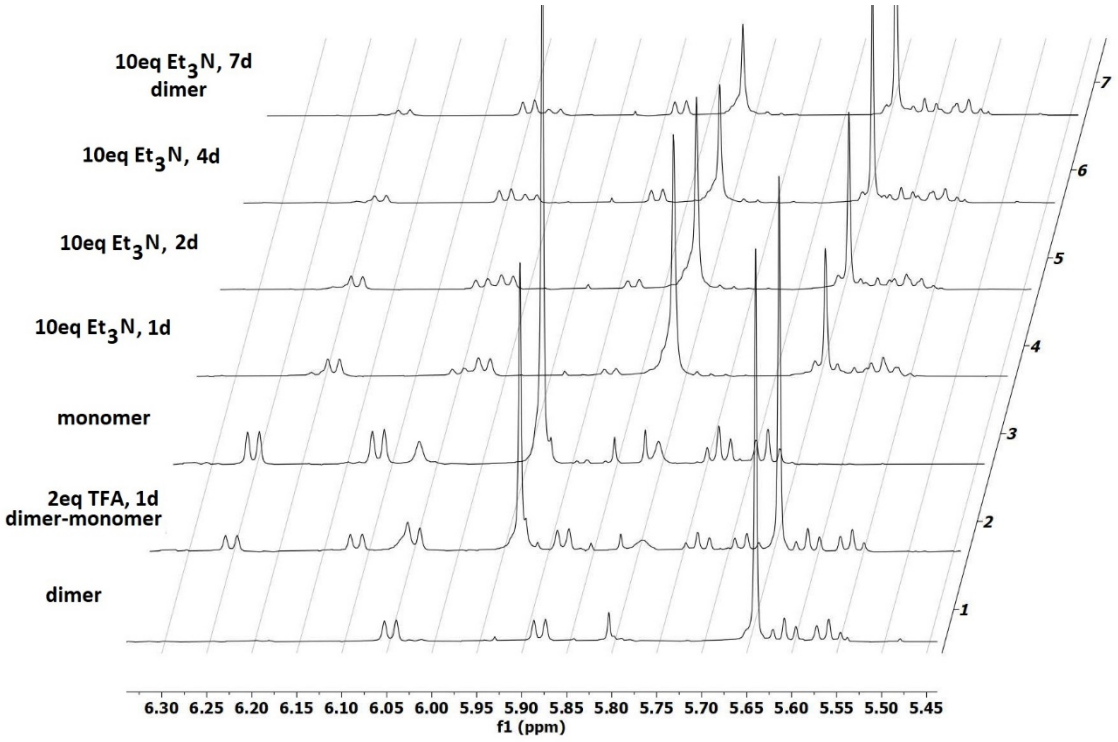

Figure S35. Waterfall plot of reversible dimer-monomer equilibrium after addition of HTFA and Et_3N. Initial concentration of $\mathbf{[(4b)_2]^{2+}}$ is 1.11 mM.

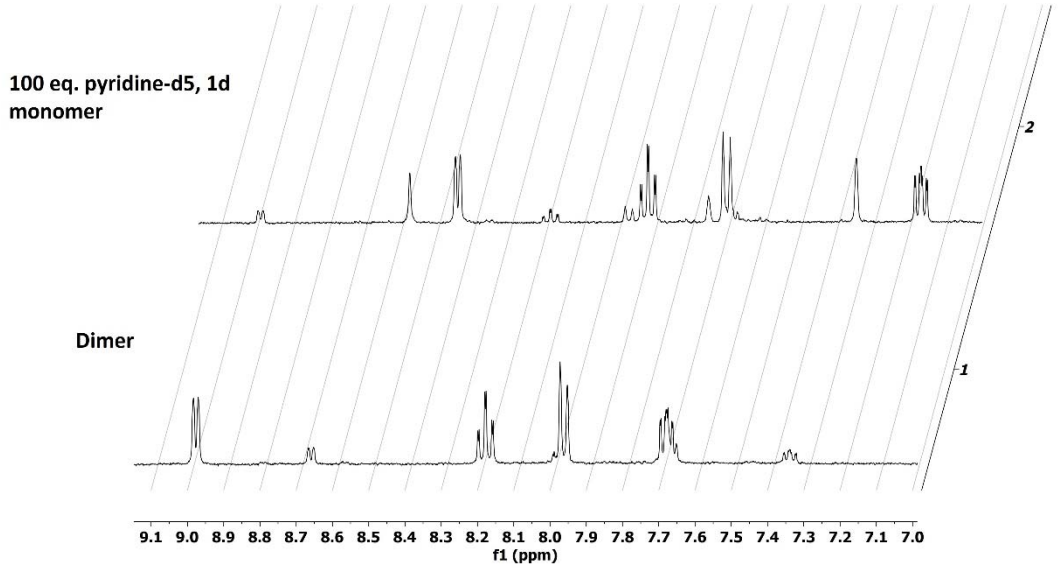

Figure S36. Dimer-monomer equilibrium after addition of 100 eq. pyridine-d5. The initial sample of the dimer contains already a small portion of monomer where the acetonitrile-d3 coordinates the Ru^{II} center. A new type of monomer is observed after addition of pyridine-d5.

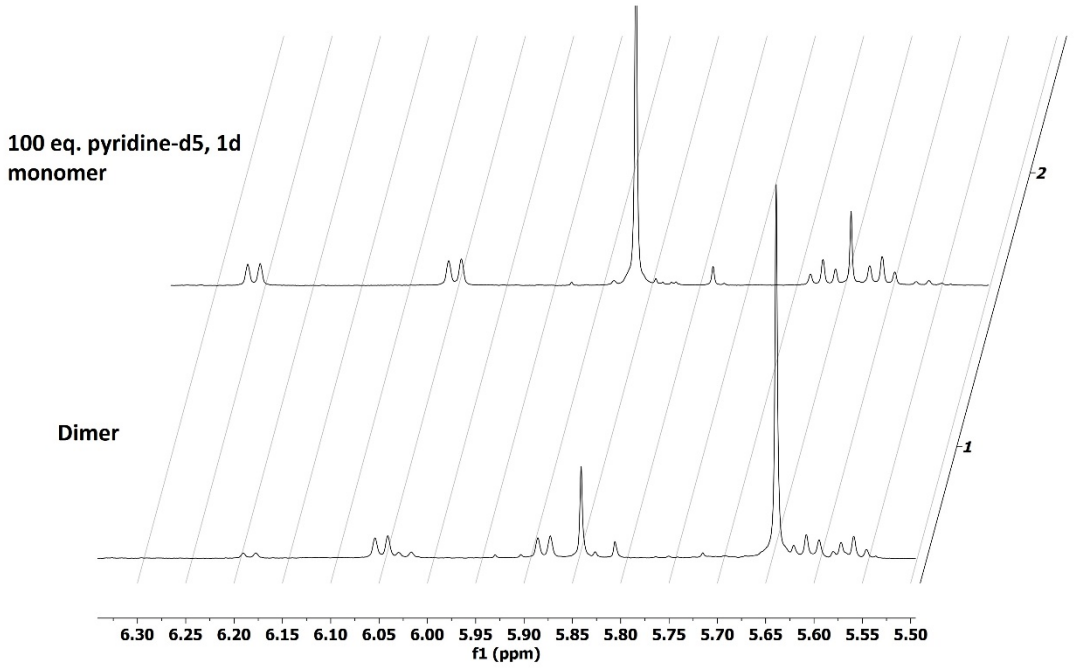

Figure S37. Dimer-monomer equilibrium after addition of 100 eq. pyridine-d5. The initial sample of the dimer contains already a small portion of monomer where the acetonitrile-d3 coordinates the Ru^{II} center. A new type of monomer is observed after addition of pyridine-d5.

Table S1. Observed rate constants (k_{obs}) for the formation of (±)-**(4b)**$^{+}$ at different concentrations of HTFA in ACN-d3 at 298 K.

HTFA [mM]	k_{obs} [s^{-1}]
111	0.000868
138	0.00111
166	0.00144
179	0.00151
193	0.00161
207	0.00170

6. DFT calculations

All calculations were performed using the Gaussian 09, Revision D.01 software.[6] The geometry of all complexes was optimized using Density Functional Theory (DFT). The calculations were carried out at the IEFPCM(MeCN)/B3LYP level of theory, with LANL2DZ[7] as effective core potential basis set for rhenium and ruthenium, and a 6-311G(d,p) basis set for the light atoms. Convergence to a minimum on the ground-state PES was confirmed by the absence of negative frequencies in the subsequent vibrational analysis. For comparison with experimental FTIR data, the frequencies were scaled by 0.967.

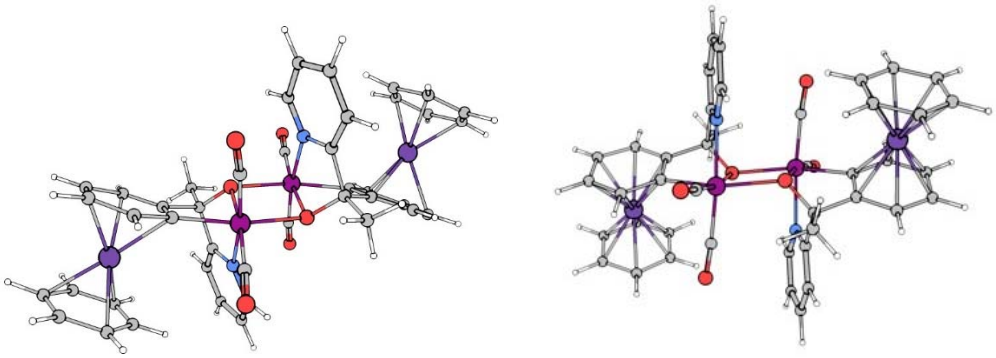

Figure S38. Representation of DFT optimized structures of complexes **[(4a)$_2$]$^{2+}$** (left) and **[(4b)$_2$]$^{2+}$** (right).

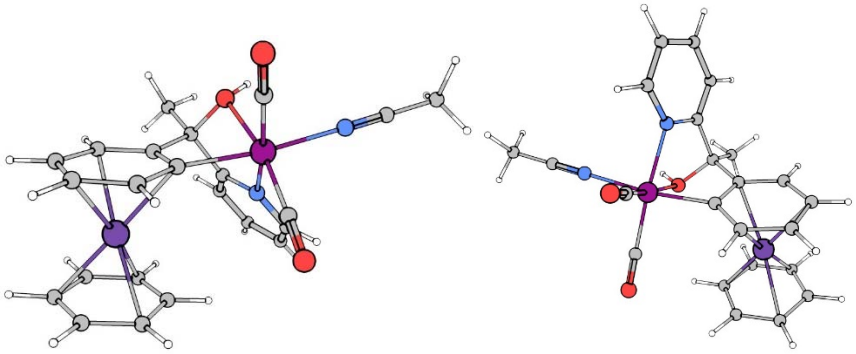

Figure S39. Representation of DFT optimized structures of complexes (*S*)-**4a**$^{+}$ (left) and (*R*)-**4b**$^{+}$ (right).

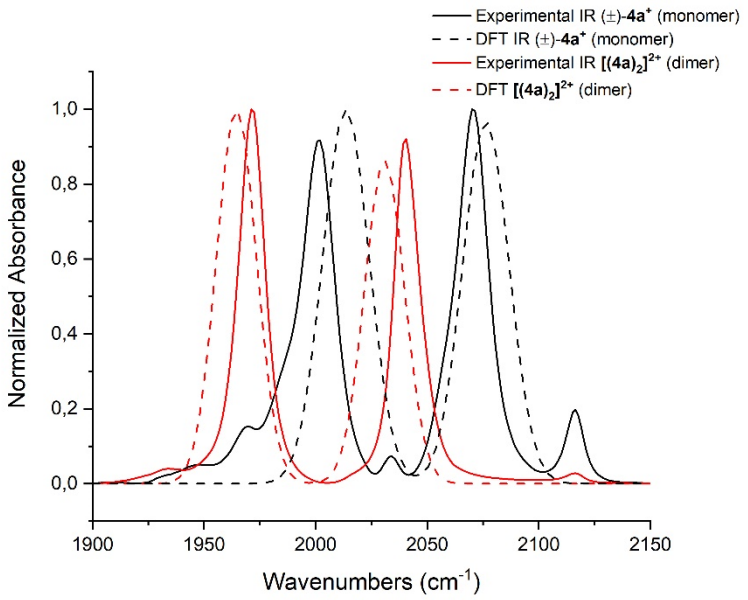

Figure S40. DFT-calculated vs experimental IR spectra in solution (ACN). IR spectra of (±)-**4a**$^{+}$ (black) and **[(4a)$_2$]**$^{2+}$ (red) are shown as continuous lines. IR absorptions calculated by DFT are shown as dashed lines. Calculated spectra resulted from a convolution of a Lorentzian function with 8 cm^{-1} FWHM. The frequencies are plotted against the normalized absorbance.

7. Crystallographic data

Table S2. Crystal data and data collection of complexes (±)-**[4a]**(TFA) and (±)-**[4b]**(TFA).

	(±)-**[4a]**(TFA)	(±)-**[4b]**(TFA)
Empirical formula	$C_{25}H_{18}F_6NO_7ReRu$	$C_{25}H_{18}F_6NO_7ReRu$
Diffractometer	XtaLAB Synergy, Dualflex, Pilatus 200 K	XtaLAB Synergy, Dualflex, Pilatus 200 K
Wavelength (Å)	Cu Kα (λ = 1.54184)	Cu Kα (λ = 1.54184)
mol. weight (g/mol)	845.67	845.67
Crystal system	monoclinic	monoclinic
Space group	$P2_1/n$	$P2_1/n$
a (Å)	12.5216(2)	10.55040(10)
b (Å)	12.3888(2)	17.4219(2)
c (Å)	16.6363(3)	14.64830(10)
α (°)	90	90
β (°)	102.256(2)	102.8060(10)
γ (°)	90	90
Volume ($Å^3$)	2521.93(8)	2625.50(4)
Z	4	4
Dens.(calc.) (g/cm^3)	2.227	2.139
Abs. coeff. (mm^{-1})	14.949	14.359
F(000)	1616.0	1616.0
Crystal size (mm^3)	0.089 × 0.082 × 0.017	0.121 × 0.046 × 0.027
Crystal description	brown plate	brown needle
2θ range (°)	8.068 to 159.838	8.004 to 159.112
Index ranges	-15 ≤ h ≤ 15, -15 ≤ k ≤ 15, -21 ≤ l ≤ 21	-13 ≤ h ≤ 13, -21 ≤ k ≤ 22, -18 ≤ l ≤ 18
Refl. collected	49374	56056
Indep. reflections	5442 [Rint = 0.0834]	5651 [Rint = 0.0399]
Reflections obs.	4847	5443
Criterion for obs.	>2sigma(I)	>2sigma(I)
Completeness to θ	98.9 to 79.92°	99.98 to 74.33°
Absorption corr.	Multi-scan	gaussian
Max. and min. transm.	1.000 and 0.727	0.914 and 0.294
Data / restraints / param.	5442/3/374	5651/3/404
Goodness-of-fit on F^2	1.085	1.089
Fin. R ind. [I>2sigma(I)]	R1 = 0.0413, wR2 = 0.1078	R1 = 0.0320, wR2 = 0.0829
R indices (all data)	R1 = 0.0456, wR2 = 0.1101	R1 = 0.0332, wR2 = 0.0838
Fin. diff. ρ_{max} ($e^-/Å^3$)	2.27 and -1.36	2.23 and -0.89

Table S3. Crystal data and data collection of complex **[(4b)$_2$]**PF_6.

	[(4b)$_2$](PF_6)
Empirical formula	$C_{42}H_{34}F_{12}N_2O_6P_2Re_2Ru_2$
Diffractometer	XtaLAB Synergy, Dualflex, Pilatus 200 K
Wavelength (Å)	Cu Kα (λ = 1.54184)
mol. weight (g/mol)	1527.19
Crystal system	triclinic
Space group	P-1
a (Å)	9.53370(10)
b (Å)	10.99430(10)
c (Å)	11.15720(10)
α (°)	99.0170(10)
β (°)	103.0770(10)
γ (°)	102.8080(10)
Volume (Å^3)	1084.116(19)
Z	1
Dens.(calc.) (g/cm^3)	2.339
Abs. coeff. (mm^{-1})	17.812
F(000)	724.0
Crystal size (mm^3)	0.181 × 0.044 × 0.032
Crystal description	needle
2θ range (°)	8.336 to 158.906
Index ranges	-11 ≤ h ≤ 11, -14 ≤ k ≤ 14, -14 ≤ l ≤ 14
Refl. collected	41894
Indep. reflections	4611 [Rint = 0.0486]
Reflections obs.	4330
Criterion for obs.	>2sigma(I)
Completeness to θ	99.86 to 74.33°
Absorption corr.	gaussian
Max. and min. transm.	1.000 and 0.348
Data / restraints / param.	4611/0/308
Goodness-of-fit on F^2	1.074
Fin. R ind. [I>2sigma(I)]	R1 = 0.0254, wR2 = 0.0669
R indices (all data)	R1 = 0.0270, wR2 = 0.0678
Fin. diff. ρmax (e$^-$/Å^3)	1.93 and /-1.15

8. References

1. CrysAlisPro Software system; Rigaku Oxford Diffraction, vers. 1.171.40; Rigaku Corporation, 2019.
2. G. M. Sheldrick, *Acta Cryst. A*, 2015, **71**, 3-8.
3. G. M. Sheldrick, *Acta Cryst. C*, 2015, **71**, 3-8.
4. A. Spek, *J. Appl. Crystallogr.*, 2003, **36**, 7-13.
5. M. Cleare and W. Griffith, *J Chem. Soc. A*, 1969, 372-380.
6. Gaussian 09, Revision D.01, M. J. Frisch, G. W. Trucks, H. B. Schlegel, G. E. Scuseria, M. A. Robb, J. R. Cheeseman, G. Scalmani, V. Barone, G. A. Petersson, H. Nakatsuji, X. Li, M. Caricato, A. Marenich, J. Bloino, B. G. Janesko, R. Gomperts, B. Mennucci, H. P. Hratchian, J. V. Ortiz, A. F. Izmaylov, J. L. Sonnenberg, D. Williams-Young, F. Ding, F. Lipparini, F. Egidi, J. Goings, B. Peng, A. Petrone, T. Henderson, D. Ranasinghe, V. G. Zakrzewski, J. Gao, N. Rega, G. Zheng, W. Liang, M. Hada, M. Ehara, K. Toyota, R. Fukuda, J. Hasegawa, M. Ishida, T. Nakajima, Y. Honda, O. Kitao, H. Nakai, T. Vreven, K. Throssell, J. A. Montgomery, Jr., J. E. Peralta, F. Ogliaro, M. Bearpark, J. J. Heyd, E. Brothers, K. N. Kudin, V. N. Staroverov, T. Keith, R. Kobayashi, J. Normand, K.

Raghavachari, A. Rendell, J. C. Burant, S. S. Iyengar, J. Tomasi, M. Cossi, J. M. Millam, M. Klene, C. Adamo, R. Cammi, J. W. Ochterski, R. L. Martin, K. Morokuma, O. Farkas, J. B. Foresman, and D. J. Fox, Gaussian, Inc., Wallingford CT, 2016.

7. T. H. Dunning Jr, *J. Chem. Phys.*, 1989, **90**, 1007-1023.